Nanostructured boron nitride–based materials: synthesis and applications

D. Gonzalez-Ortiz, C. Salameh, Mikhael Bechelany, P. Miele

Materials Today Advances 8 (2020) 100107

Contents lists available at ScienceDirect

Materials Today Advances

journal homepage: www.journals.elsevier.com/materials-today-advances/

Nanostructured boron nitride–based materials: synthesis and applications

D. Gonzalez-Ortiz [a], C. Salameh [a], M. Bechelany [a], P. Miele [a, b, *]

[a] Institut Européen des membranes, IEM UMR 5635, Univ Montpellier, CNRS, ENSCM, Montpellier, France
[b] Institut Universitaire de France, IUF, 1 Rue Descartes, 75231, Paris cedex 5, France

ARTICLE INFO

Article history:
Received 10 June 2020
Received in revised form
7 August 2020
Accepted 12 August 2020
Available online 10 October 2020

Keywords:
BN
Nanocomposites
Energy
Health
Environment

ABSTRACT

Nanocomposite materials are widely studied because of their unique design opportunities and properties. They can be classified into three main groups in function of the matrix used: polymer-based, ceramic-based, and metal-based nanocomposites. The nanofiller choice is one of the most important steps because it will improve the nanocomposite properties. This review focuses on boron nitride as nanofiller because of its extraordinary properties: high thermal and chemical stability, good mechanical strength, superior resistance to oxidation, good thermal conductivity, and electrical insulation. The goal of this review is to provide an overview on the synthesis methods to produce boron nitride–based nanocomposites, particularly polymer- and ceramic-based nanocomposites, and on their potential applications in promising fields, such as energy, environment, and health.

1. Introduction

Nanostructured materials refer to materials with nanometer-scale size in one, two, or three dimensions and one dimension in the 1–100 nm range. Over the last years, these materials have attracted the scientists' interest because of their remarkable physicochemical, electrical, and biological properties that allow a wide range of applications in different fields (e.g. energy, environment, and health) [1]. Their addition in a matrix can enhance the bulk material's properties.

Among nanostructured materials, the interest for boron nitride (BN)–based materials has progressively increased because of their high chemical stability, mechanical strength, resistance to oxidation, thermal conductivity, and electrical insulation [2]. BN contains an equal number of boron (B) and nitrogen (N) atoms. BN is isostructural to graphite; however, the N atomic nucleus and B atoms combine an sp^2 orbital to form a strong σ bond. Furthermore, it presents a partially ionic character because of the electron pairs in sp^2 hybridized B–N and weak van der Waals forces between B and N atoms of adjacent layers, thus providing anisotropic properties. BN exists in four crystalline forms: hexagonal BN (h-BN), cubic BN (c-BN), rhombohedral BN (r-BN), and wurtzite BN (w-BN). The main difference among these phases is the hybridization: h-BN and r-BN are dense phases with sp^2 hybridization, whereas c-BN and w-BN are low-density phases with sp^3 hybridized B–N bonds [3]. Among them, h-BN is particularly interesting because of its structural analogy with graphite [4]. BN nanomaterials can be zero-dimensional (0D; e.g. nanospheres), one-dimensional (1D; e.g. nanotubes, nanofibers, and nanoribbons), two-dimensional (2D; e.g. thin films and nanosheets [5]), and three-dimensional (3D; e.g. nanostructured porous materials) (Fig. 1). Low-dimensional materials show quantum confinement and interfacial effects compared with micro- and macro-scale materials. Unique physical and chemical properties, such as wide band gap (~5.5 eV), high chemical and thermal stability, and excellent electric insulation, can be obtained by combining the low-dimensional quantum confinement and surface effects of BN. Therefore, h-BN is a promising scaffold for functional materials and for many potential applications, such as electronics [6,7], sensors [8,9], hydrogen storage [10,11], health [12,13], and also water and gas separation [14–19].

During the last 10 years, several reviews have been published on the synthesis, functionalization methods, and potential applications of low-dimensional BN-based materials. Golberg et al. [20] published a concise review on the history of low-dimensional BN nanomaterials, particularly on the synthesis methods (e.g. chemical vapor deposition, ball milling, chemical exfoliation) of 1D and 2D

* Corresponding author.
E-mail address: philippe.miele@umontpellier.fr (P. Miele).

https://doi.org/10.1016/j.mtadv.2020.100107

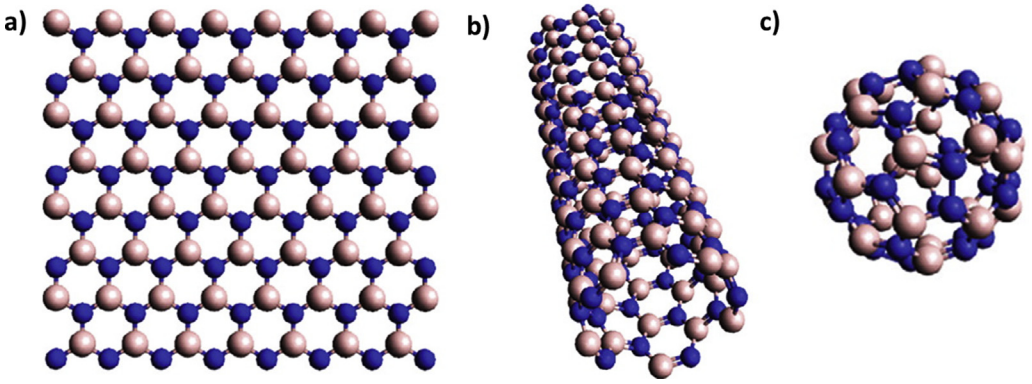

Fig. 1. Structural models of low-dimensional BN nanostructures: (a) single-layered nanosheet (2D), (b) single-walled nanotube (1D), and (c) single-shelled fullerene (0D). Reprinted with permission from Ref. [20]. Copyright © 2012, Elsevier Ltd.

BN-based materials, their morphology, and applications. Miele et al. [21,22] reviewed the advances in the synthesis of nanostructured BN from polymeric precursors containing boron, nitrogen, and hydrogen. They also discussed their potential applications and future perspective for their synthesis and applications. Weng et al. [23] described the structural features as well as physical and chemical properties of functionalized h-BN nanomaterials. They also discussed the different strategies to functionalize BN, including physical and chemical routes, their emerging properties, and applications. Wang et al. [3] described the synthesis, structure, properties, and applications of graphene and h-BN materials. They focused on the mechanical, optical, thermal, electric, and magnetic features of these 2D materials. Wang et al. [24] published a general overview on environmental restoration using BN-based materials for pollutant elimination. They presented recent advances on the removal of organic/inorganic pollutants using BN-based materials, and described the underlying interaction mechanisms. Indeed, BN-based materials show high sorption capacity and good removal performances of heavy metal ions and organic pollutants from aqueous solutions because of their high surface areas and chemical inertness.

The aim of this review is to summarize the most recent advances in BN-based nanocomposites. First, the methods used for their synthesis in function of the chosen matrix (polymer or ceramic) will be discussed. Then, their applications in the fields of energy, environment, and health will be presented (Fig. 2).

2. Nanocomposite synthesis methods

Nanocomposites are new composite materials in which at least one of the constituents has nanometric dimensions. The matrix is generally massive and the strengthening nanometric. Nanofillers are added to improve the mechanical, thermal, and physicochemical properties of the resulting materials [25]. The ideal situation for

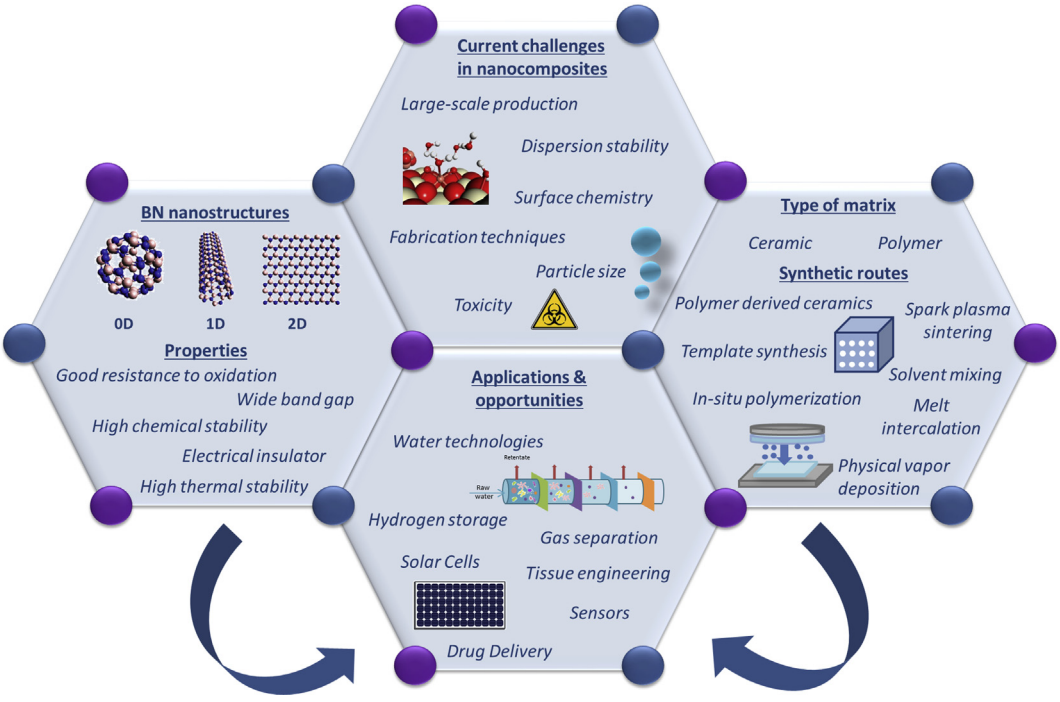

Fig. 2. Schematic summary on current challenges of BN nanocomposites. Type of BN nanostructures and their properties, synthesizing strategies for polymer- and ceramic-based nanocomposites and their applications/opportunities.

nanocomposite synthesis involves uniform dispersion of the nanofillers in a polymer or ceramic matrix even if metallic matrices may also be used. The uniform dispersion can lead to large interface areas between the nanocomposite components. Nanocomposites are classified according to the types of nanofillers and matrix materials used. Here, two main classes of BN nanocomposites will be discussed in function of the chosen matrix material: polymer- and ceramic-based nanocomposites.

2.1. Polymer-based nanocomposites

Polymer-based nanocomposites are materials with a polymer matrix that serves as host for material and nanofillers (i.e. BN nanomaterials) that are used as reinforcement. Polymers display interesting properties, such as light weight, easy processing, resistance to corrosion, ductility, and low cost as well as gas barrier properties, heat resistance, and fire resistance [26,27]. Their main drawback is their low thermal and electrical conductivities [28]. Adding nanofillers as reinforcing agents into a polymer matrix enhances significantly the properties of the fabricated nanocomposite. As mentioned earlier, nanofillers can be classified into three classes depending on their dimensionality: 0D (i.e. spherical particles), 1D (i.e. nanotubes and fibers), and 2D (i.e. nanosheets). The development of novel polymer nanocomposites with enhanced properties depends on many parameters, such as the nanofiller shape, the dispersion, the morphology, and the external stimulus (Fig. 3) [29]. The choice of reinforcement material is based on the targeted application. Several factors play a major role in the polymer matrix reinforcement: (i) the matrix nature; (ii) the nanofiller nature and concentration; and (iii) the average particle size, orientation, and distribution [30].

In the early 1990s, Kamigaito et al. [31,32] synthesized polymer nanocomposites by producing a nylon 6-clay hybrid through one-pot synthesis by intercalation of silica with ε-caprolactam and further polymerization of ε-caprolactam. Nowadays, polymer nanocomposites are synthesized using various methods that can be categorized into four major routes: melt intercalation/blending, *in-situ* polymerization intercalation, template synthesis, and solvent mixing. More recently, sonication and high-shear mixing have been proposed as alternative techniques to prepare (bio)-nanocomposite materials. This review will focus on the methods to obtain polymer-based nanocomposites using h-BN as nanofillers to enhance their properties.

2.1.1. Melt intercalation/blending

Melt intercalation is the most used approach for the synthesis of thermoplastic polymer-based nanocomposites. This approach generally involves three steps: polymer matrix annealing at high temperatures, nanofiller addition, and composite blending to obtain a homogeneous distribution [33]. For instance, h-BN can be incorporated into a polymer matrix by preparing thermoplastic polyurethane (TPU) nanocomposites that contain nano-h-BN by melt blending using co-rotating twin screw extruder and hot pressing techniques to obtain thin TPU/h-BN films. Kahraman et al. [34] demonstrated that h-BN addition increases the nanocomposite mechanical strength and thermal conductivity. Öner et al. [35] studied the effect of h-BN nanoparticle incorporation into poly (3-hydroxybutyrate-*co*-3-hydroxyvalerate) (PHBV), a derivate of biodegradable and bio-sourced thermoplastic polyester. PHBV is very brittle and display low thermal stability. The authors demonstrated that h-BN incorporation into the matrix by melt mixing increases the nanocomposite oxygen barrier and thermal properties. Wang et al. [36] improved nylon-6 (PA6) thermal conductivity and mechanical properties through a two-step reaction in which surface functionalization of BN nanosheets (BNNS) with amino groups was followed by melt blending with PA6. As amino-functionalized BNNSs are better dispersed in the matrix than non-functionalized BNNSs (Fig. 4), the thermal conductivity and thermal stability of PA6/A-BNNS nanocomposites were improved by nearly 10 times.

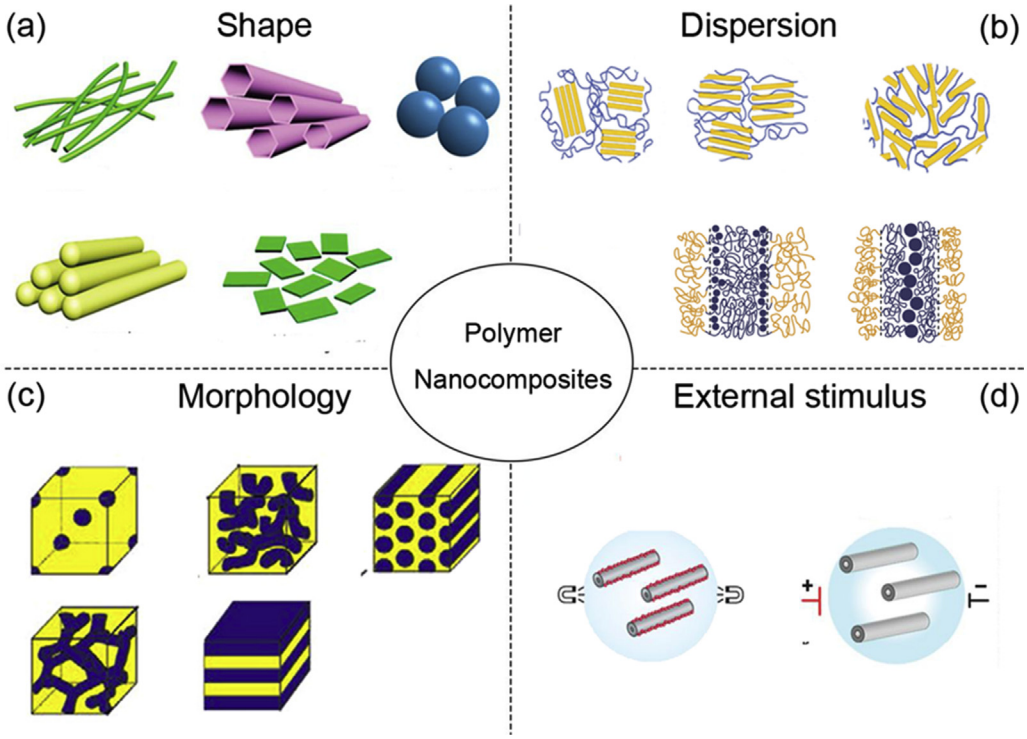

Fig. 3. Research on polymer nanocomposites has focused on (a) shape, (b) dispersion, (c) morphology, and (d) external stimulus. Reproduced with permission from Ref. [29].

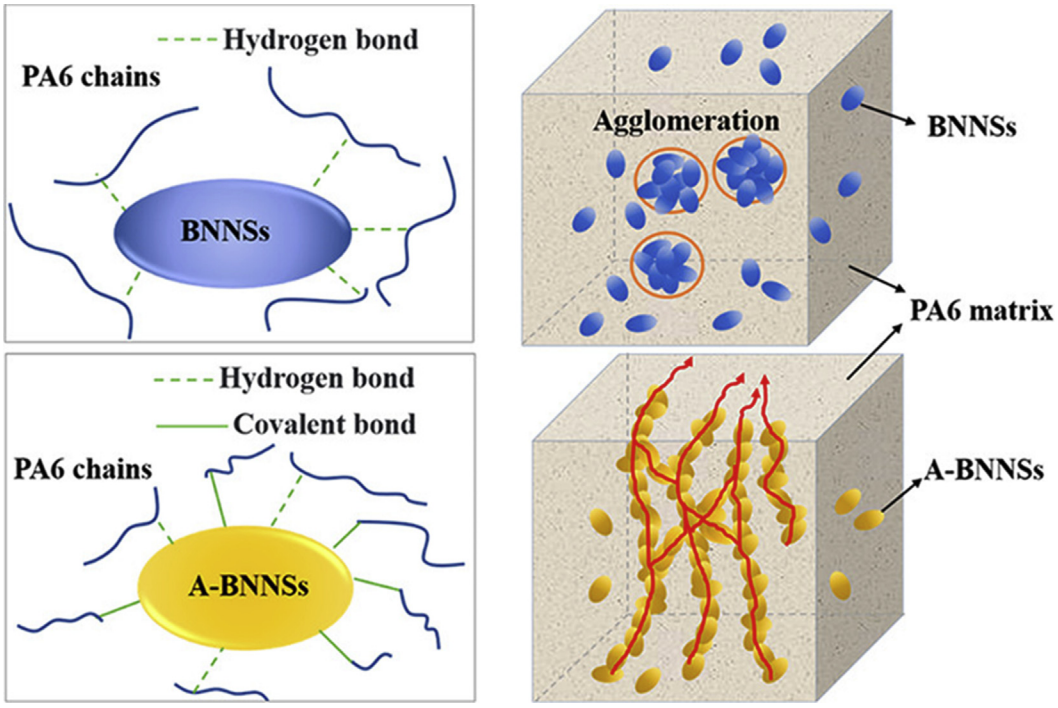

Fig. 4. Nanocomposites made of nylon-6 (PA6) and h-BNNS or amino functionalized h-BNNS (A-BNNS). Reprinted with permission from Ref. [36]. Copyright © 2018, American Chemical Society.

2.1.2. In-situ polymerization

In-situ polymerization allows the effective dispersion of nanofillers in the polymer matrix. Generally, nanomaterials are mixed into a neat monomer (or monomer solution) that is then polymerized using heat, radiation, or an organic initiator. Therefore, this method presents some advantages for preparing BN/polymer-based nanocomposites, particularly the strong interaction between BN nanoparticles and polymer matrix due to covalent bonds, and the suppression of particle aggregation due to the controllable growth of polymer chains. However, more research is needed on solvent removal. Huang et al. [37] designed a reversible addition fragmentation chain transfer polymerization method to prepare thermally conductive polystyrene (PS)/BN nanosphere nanocomposites by initiating styrene macromolecular chains on the surface of amino-functionalized BN nanospheres. Compared with non-functionalized BN composites, the prepared BN nanospheres@PS nanocomposites display higher thermal conductivity and dielectric properties. The in-situ polymerization approach was also used to prepare self-healing materials with improved self-healing efficiency. Briefly, micron-sized BN (mBN) filler was introduced in the system during the polymerization of thiol-epoxy elastomers. The obtained mBN/thiol epoxy elastomer nanocomposites with different mBN loads showed higher self-healing performance and better mechanical and thermal properties [38]. Wang et al. [39] used a double strategy to produce a 3D BN network in a PS matrix. First, they prepared styrene oil droplets in water stabilized by BN to form Pickering emulsions, and then they used in-situ polymerization to synthesize PS microspheres with an ultrathin BN layer at the surface. Finally, they produced nanocomposites based on BN networks by hot-pressing PS@BN microspheres (Fig. 5).

2.1.3. Template synthesis

Templating is one of the most important techniques to produce nanostructured materials; it uses a pattern as a guide to form the nanocomposite structure. Generally, the nanomaterials synthesized with this method display well-defined size, shape, and configuration. Templating to fabricate nanostructured materials involves three main steps: (i) building block creation, (ii) building block directed assembly, and (iii) template removal (if necessary) [40]. There are mainly three template types to produce nanostructured materials: colloidal templates, soft templates, and other non-colloidal templates. Zeng et al. described a method to develop 3D-BNNS networks using an ice-templated approach. First, they performed anisotropic freezing using liquid nitrogen as cryogen by pouring the non-functionalized BNNS (NF-BNNS) aqueous slurry into a Teflon mold. During freezing, the suspended NF-BNNS and polyvinyl alcohol (PVA) were expelled from the growing ice crystals and this allowed controlling the ice growth direction (Fig. 6). Then, the frozen samples were freeze-dried to obtain the BNNS aerogel scaffolds. This was followed by 3D-BNNS aerogel sintering and immersion in an epoxy solution matrix where the resin infiltrated the aerogel scaffold to obtain 3D-BNNS aerogel nanocomposites [41]. This strategy opens new routes for green template synthesis because of the limited use of organic solvents. Gonzalez Ortiz et al. used the Pickering emulsion method as soft templating strategy to produce porous structured PVA/h-BN nanosheet (h-BNNS) nanocomposites. Importantly, the addition of h-BNNS to a polymeric matrix using Pickering emulsion method avoids nanosheet aggregation. h-BNNS are irreversibly adsorbed at the water–oil interface, and the nanostructured PVA/h-BNNS films are obtained after the removal of the oil phase [19]. Producing nanocomposites with the emulsion templating approach is interesting because it avoids several sintering steps and it does not require harmful solvents [42].

2.1.4. Solvent mixing

The solvent mixing method allows the dispersion of nanofillers, mainly layered materials, into the polymer matrix nanocomposites. In this approach, nanofillers are exfoliated by intercalation of an

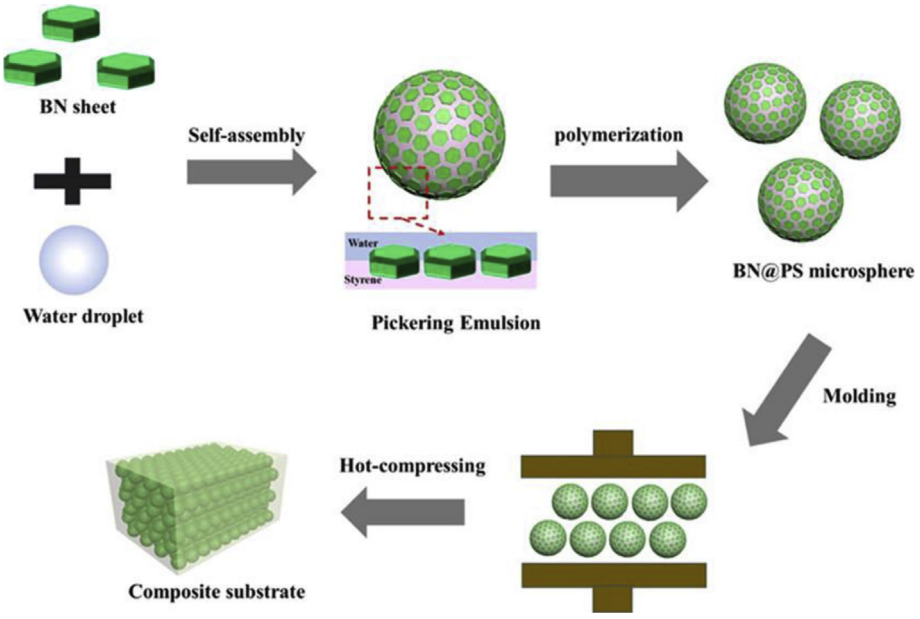

Fig. 5. Schematic representation of BN@PS nanocomposite preparation by in-situ polymerization of Pickering emulsions. Reprinted with permission from Ref. [39]. Copyright © 2019, American Chemical Society.

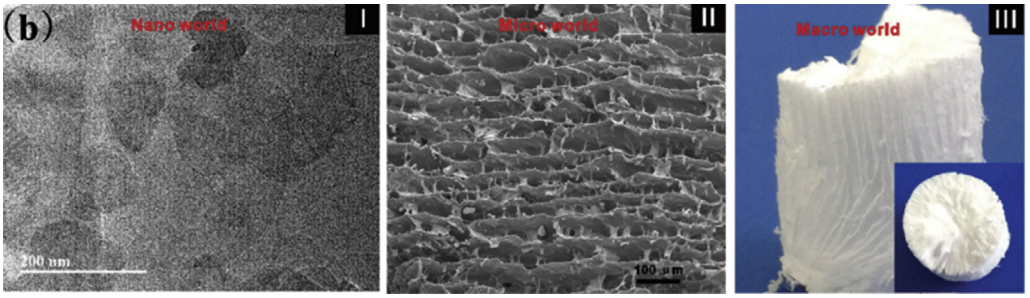

Fig. 6. Hierarchical structures of the free-standing 3D-BNNS aerogel: (I) transmission electron microscopy image of the BNNS; (II) scanning electron microscopy image of the 3D-BNNS aerogel in the direction perpendicular to the ice growth; (III) photograph of a 3D-BNNS aerogel. Reprinted with permission from Ref. [41]. Copyright © 2016, WILEY-VHC Verlag GmbH & Co. KGaA, Weinheim.

organic compound into the nanofiller interlayer space, resulting in well-dispersed plate-like particles. Then, the exfoliated material is dispersed in a solvent and mixed with the polymer solution. The polymer chains intercalate and displace the solvent within the layered material, and after solvent removal, a multilayered structure that contains the polymer chains trapped in the structure is obtained. The as-resulting nanocomposites are reinforced because of the large contact surface area between matrix and exfoliated material. The polymer intercalation approach is also used to prepare BN-based polymer nanocomposites with improved thermal conductivity and mechanical strength [43].

As BNNSs display a 2D structure, they can be easily oriented along the plane in polymer matrices. This property has been exploited to fabricate nanocomposites with higher thermal conductivity using the polymer intercalation method. Song et al. [44] described the production of BNNSs by dispersion in polymers to obtain composite films with very good thermal transport performances, similar to those of polymer/graphene nanocomposites. Morishita et al. [45] prepared NF-BNNS/thermoplastic polymer composite films using a simple wet-process method. First, they prepared exfoliated NF-BNNS from h-BN by physical adsorption of chlorosulfonic acid on the h-BN surfaces via sonication. Then, the NF-BNNSs were dispersed in acetone and mixed with a poly (methyl methacrylate)/acetone solution. The nanocomposite was obtained after spreading the solution onto a glass support.

Following the same strategy of nanofiller alignment, poly(-vinylidene fluoride-chlorotrifluoroethylene) (P(VDF-CTFE)) nanocomposites with parallel BNNSs embedded in a polymer matrix were prepared by casting. First, h-BN was exfoliated using fluoro-hyperbranched polyethylene-graft-poly(trifluoroethyl methacrylate) as the polymer stabilizing agent to avoid nanosheet aggregation. Then, the resulting BNNSs were dispersed in dimethylformamide and the dispersion was added to a P(VDF-CTFE) matrix to prepare BNNS/P(VDF-CTFE) nanocomposite films. Finally, to tune the nanosheet orientation along the direction of deformation, the films were uniaxially stretched at a constant temperature (Fig. 7) [46]. Similarly, gelatin-graphene-like BN nanobiocomposites were fabricated in which h-BN addition improved their mechanical properties. The as-prepared h-BN/gelatin materials displayed gas barrier properties, and good barrier performance for O_2 [27].

This section gave an overview of the different methods to prepare polymer-based nanocomposite materials. Each technique has its own advantages and drawbacks, and the perfect method does not exist. The method must be chosen and adjusted in function of the target application, composition,

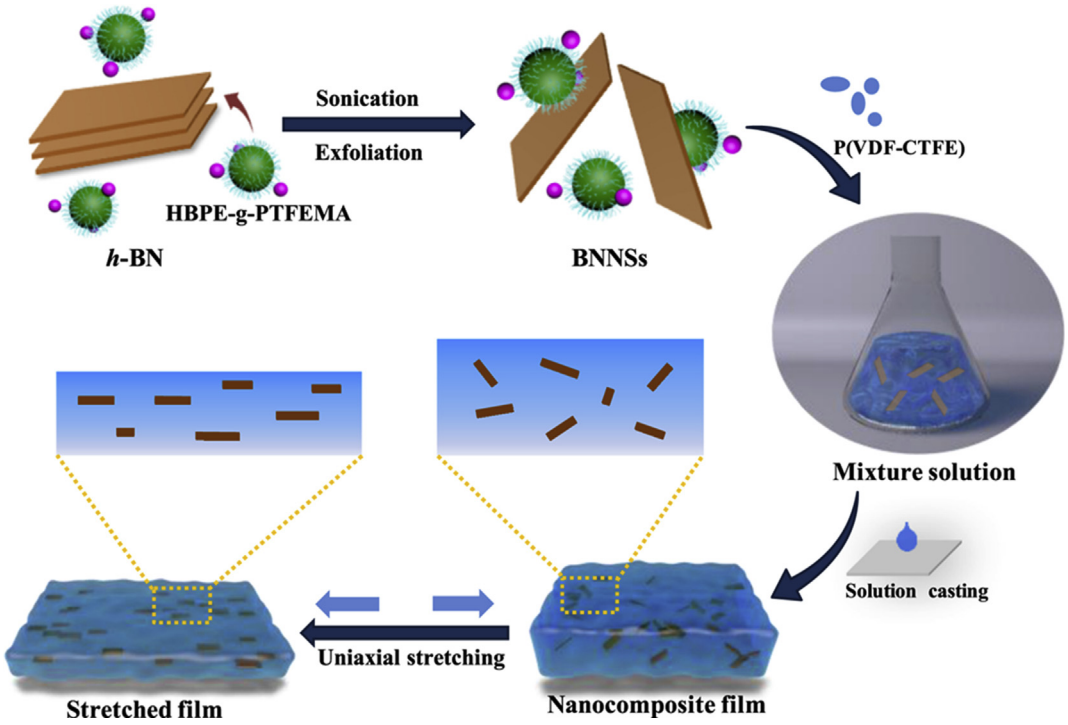

Fig. 7. Schematic illustration of liquid-phase BNNS exfoliation in dimethylformamide using fluoro-hyperbranched polyethylene-graft-poly(trifluoroethyl methacrylate) (HBPE-g-PTFEMA) and of the preparation of the stretched BNNS/P(VDF-CTFE) nanocomposite film. Reprinted with permission from Ref. [46]. IOP Publishing, Ltd.

dispersion performance, and so on. The uniform dispersion of nanofillers in polymer matrices is a general prerequisite for achieving the desired mechanical and physical characteristics. The nanocomposite mechanical properties can be influenced by different parameters, such as the matrix properties, the filler properties and distribution, as well as the processing methods. In terms of process improvements, ultrasonic-assisted dispersion has given encouraging results concerning the dispersion of nanofillers into the polymer matrix. The high-shear mixing and ball milling methods might help to improve the nanofiller dispersion. Moreover, ball milling does not require high temperatures or solvents, thus making composite preparation greener and also more convenient and effective [47]. Other techniques can be used to prepare nanostructured composites, such as 3D printing that allows the direct shaping of the polymer/nanofiller mixture to obtain nanocomposites with the desired architecture. Using Pickering emulsions as soft template approach allows regulating the internal porosity by controlling the nanofiller size and concentration and the continuous and dispersing phase volumes.

The nanocomposite properties are also influenced by the polymer matrix chemistry and the nanofiller nature. The interfaces may affect the effectiveness of load transfer from the polymer matrix to the nanofillers. Thus, surface functionalization might improve the nanofiller dispersion and enhance the interfacial adhesion between matrix and fillers.

2.2. Ceramic-based nanocomposites

Ceramics have been investigated as candidate structural materials to be used in conditions (e.g. temperature, loading rates, wear, and chemical aggression) that are too severe for polymers and metals. However, the major drawback of ceramics is their intrinsic brittleness that prevents their use in many real-life applications. Therefore, much research has focused on designing a new generation of ceramics through incorporation of secondary phases (e.g. particles, fibers, or whiskers) that help to tolerate flaws by deflecting or attenuating the ceramic cracks and stress. One of the most important developments has been the production of nanocomposite ceramics in which multiple phases are distributed in the ceramic composite at the nanoscopic scale.

In their pioneering work, Niihara et al. [48] reported fracture strengths of 1.5 GPa and toughness of 7.5 MPa m^2 in systems in which nanometer-sized silicon carbide (SiC) was embedded in $A1_2O_3$, MgO, Si_3N_4, and mullite matrices. Oxide nanocomposite ceramics, such as silica (SiO_2) and alumina (Al_2O_3), have been much investigated because of their hardness, good compressive strength, good oxidation resistance, and relatively low density [49–51]. More recently, Sharma et al. [52] obtained SiO_2- and Al_2O_3-based nanocomposites with multiwalled carbon nanotubes and exfoliated graphite nanoplatelets as nanofillers by using spark plasma sintering. These nanofillers provided a better lubrication to the nanocomposites compared with monolithic SiO_2 and Al_2O_3 ceramics.

Since the work by Niihara et al. [48,53] who demonstrated large improvements in the fracture toughness and strength, SiC/silicon nitride (SiC/Si_3N_4) composites have been increasingly studied and have been shown to perform very well under high temperature oxidation. Studies on such nanocomposites have focused on advanced microstructures, such as polycrystalline SiC and Si_3N_4 nanocomposites [54] and $TiN–Si_3N_4$ [55] and $SiC–Al_2O_3$ [56] nanocomposites.

To continue exploring nanocomposite ceramics, it is now crucial to consider unconventional techniques that can improve their properties and reduce the production costs. A special class of nanocomposites has emerged in the last decade: polymer-derived ceramic (PDC) nanocomposites, particularly BN-based nanocomposites. These are very promising materials for different structural and functional applications, especially at high temperature, because of their thermal and chemical properties.

2.2.1. PDC nanocomposites

The PDC route is the technique of choice for manufacturing ceramic nanostructures and nanocomposites, particularly non oxides [57]. This chemical approach allows processing at temperatures lower than the conventional ones, and the structure, composition, shape, and properties can be tuned on demand [58]. Although this method was traditionally used to prepare SiC fibers [59,60], dense films [61], porous materials (e.g. powders, foams, aerogels [62–64]), and microporous membranes [65], it is now extended to many material types, including nanocomposites [66–68].

Ceramic nanocomposites can be produced from preceramic polymers by following mainly two approaches: (i) a two-source strategy in which nanofillers are added to the synthesized preceramic polymer, and (ii) a single-source approach in which all the elements of the final nanocomposite are incorporated at the molecular level. The key points of both approaches are related to the control of the nanoarchitecture and the stability of the nanostructures at the conditions of use. In the first approach developed by Greil et al. [69], nanofillers (active or passive) are synthesized and integrated in the subsequently developed matrix. Passive nanofillers are neutral with regards to the matrix, unlike active nanofillers that will react with the matrix or the products released during the thermal treatments. These nanofillers add new functionalities (mechanical, electrical, and magnetic) to the ceramic derived from the polymer, while limiting the polymer volume shrinkage during pyrolysis. In the second approach, co-blended polymers are synthesized by reaction of two precursors with different molecular weights, During pyrolysis, these two precursors will form nanoscale inclusions distributed homogeneously in the matrix by phase separation and precipitation on heat treatment [70]. Seyfert and Ishikawa [71,72] evaluated this route for producing metallic preceramic polymers by reaction of polysilazanes and polycarbosilanes with metallic precursors, thus developing metal carbides and nitrides. Transition-metal nitrides are generally characterized by high melting point, hardness, and wear resistance. When produced at the nanoscale, an extension of these properties is expected, and was confirmed by the synthesis of TiN/Si_3N_4 nanocomposite films [73] and TiN/Si_3N_4 monoliths [74]. Riedel and Ionescu and their colleagues [57,75,76] highlighted the great potential of Si-based structural nanocomposites for high-temperature applications, thanks to their thermal stability concerning crystallization and decomposition. The next section will describe BN nanocomposites, particularly when BN is used as matrix within the composite.

2.2.2. Boron nitride nanocomposites

BN-based nanocomposites can be obtained following the procedures described earlier. BN has been mainly used to prepare BN/SiC [77,78], BN/Si_3N_4 [79,80], and BN/Al_2O_3 [81,82] nanocomposites. However, in these systems, BN is not the matrix, but acts as reinforcement material to improve the ceramic thermomechanical properties and machinability. Studies in which BN is the matrix in the nanocomposite have also been published. Generally, the nanocomposite consists of two phases: (i) nanocrystalline metal nitride phase, in which the metal, titanium (Ti), zirconium (Zr), or hafnium (Hf), is homogeneously distributed in the (ii) BN matrix phase [83,84]. Metal BN (MBN) nanocomposites have been used in the field of ultra-hard coatings. Such nanocomposites are mostly fabricated using physical routes, such as physical vapor deposition [85]. However, for applications that need robust and durable materials, more complex shapes (e.g. monolithic structures) are required to obtain decorative, lightweight, and lubricant solid materials. The PDC route allows the efficient preparation of BN, particularly for the synthesis of polymers based on borazinic rings, that is, polymetalloborazines, with tailor-made properties for nanocomposite preparation. Polyborazylene is extensively used as BN preceramic polymer derived from borazine. Borazine was discovered by Stock et al. by thermal decomposition of diammoniate in 1926, and its laboratory synthesis was first described by Wideman and Sneddon [86,87] using metal borohydride-ammonium salt or ammonia borane as starting compounds. Miele et al. [88] worked on the development of unconventional shapes of BN-based nanocomposites. They developed a straightforward synthesis approach for MBN nanocomposites from preceramic polymers. The starting compounds were prepared by thermolysis of different BN sources and metal precursors (tetrakisdialkylaminometal). Analysis of the reaction mechanisms between BN precursors and the metal precursors to prepare polymetalloborazines showed that metal atoms are mainly considered as bridges linking borazine rings. The polymer-to-ceramic conversion occurred after direct pyrolysis of the polymetalloborazine at high temperatures during which several structural and chemical changes based on molecular rearrangements were observed. Gaseous by-products, inherently related to the molecular structure of the preceramic polymer, were released during the pyrolytic decomposition. The use of preceramic polymers as BN precursors facilitates processing before nanocomposite generation. Dip and spin coating, casting, as well as warm and cold pressing are conventional shaping techniques that can be easily applied using this route [89]. Monolith-type MBN nanocomposites were prepared by warm pressing the preceramic polymer followed by pyrolysis of the green compact. The molecular weight and structure of the preceramic polymers are key features that determine their shaping ability. For example, a high ceramic yield is a prerequisite for preparing MBN monoliths without cracking during thermal treatment [89].

Miele et al. [90] also produced carbon fiber-reinforced BN nanocomposites (C/BN) by vacuum assisted polyborazylene transfer molding followed by pyrolysis. As the obtained C/BN nanocomposites displayed high stability under air and vacuum, they are interesting candidates for vacuum technology and space applications.

2.2.3. Boron nitride nanostructures

Besides the previously mentioned BN-based nanocomposites, polymer-derived BN nanostructures have attracted the attention of many researchers [91–93]. The many BN nanoarchitectures, ranging from 0D to 3D structures, are displayed in Fig. 8. Such materials show chemical and physical properties that are different from those of bulk- and micro-sized materials.

Porous h-BN nanomaterials can be useful for catalyst support, hydrogen (H_2) storage, pollutant treatment, and also drug delivery. Porosity can be controlled through templating and non-templating strategies. Concerning template-directed synthesis, different templates (e.g. silica, zeolites, carbonaceous materials, surfactants, and block copolymers) have been frequently used [94,95]. The specific surface areas of these porous BNs can be very high (1,000 $m^2\ g^{-1}$). Salameh et al. [96] described the fabrication of BN mesoporous 3D monoliths with very high specific surface area and controlled crystallinity by replica of a highly porous activated carbon. These monoliths were used as nano-scaffolds for solid-state H_2 storage to form a nanocomposite that can liberate pure H_2 at low temperatures. Higher specific surface area values have been reached using non-templating approaches [97]. Moreover, spark plasma sintering allowed producing mechanically stable BN monoliths with a hierarchical porosity from ordered mesoporous powders without the need of sintering aids [98].

Ceramic aerogels, such as SiC, SiO_2, and Al_2O_3, are promising candidates for thermal insulation applications. However, they

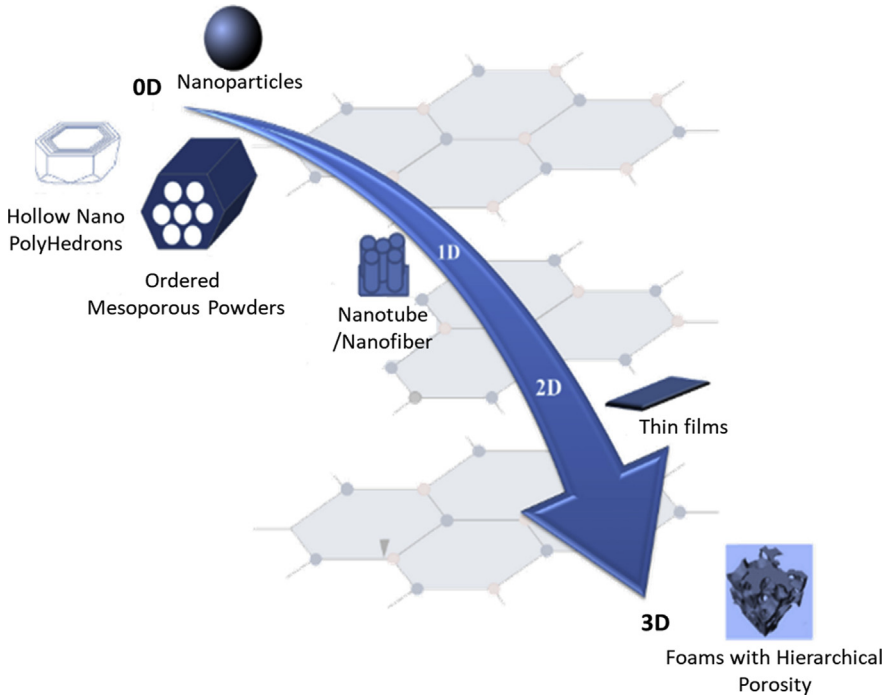

Fig. 8. Examples of different BN nanostructures. Reprinted with permission from Ref. [21].Copyright © 2014 Elsevier Ltd.

generally show poor mechanical strength and degradation under thermal shock [99,100]. Robust BN aerogels have been fabricated by Xu et al. [101] (Fig. 9) by impregnating graphene aerogels with borazine. Owing to their low thermal conductivity and very good thermal and mechanical stabilities, they overcame the drawbacks of conventional ceramic aerogels and carbonaceous materials.

Finally, the PDC approach, by molecularly engineering a family of preceramic polymers that are specifically organized for

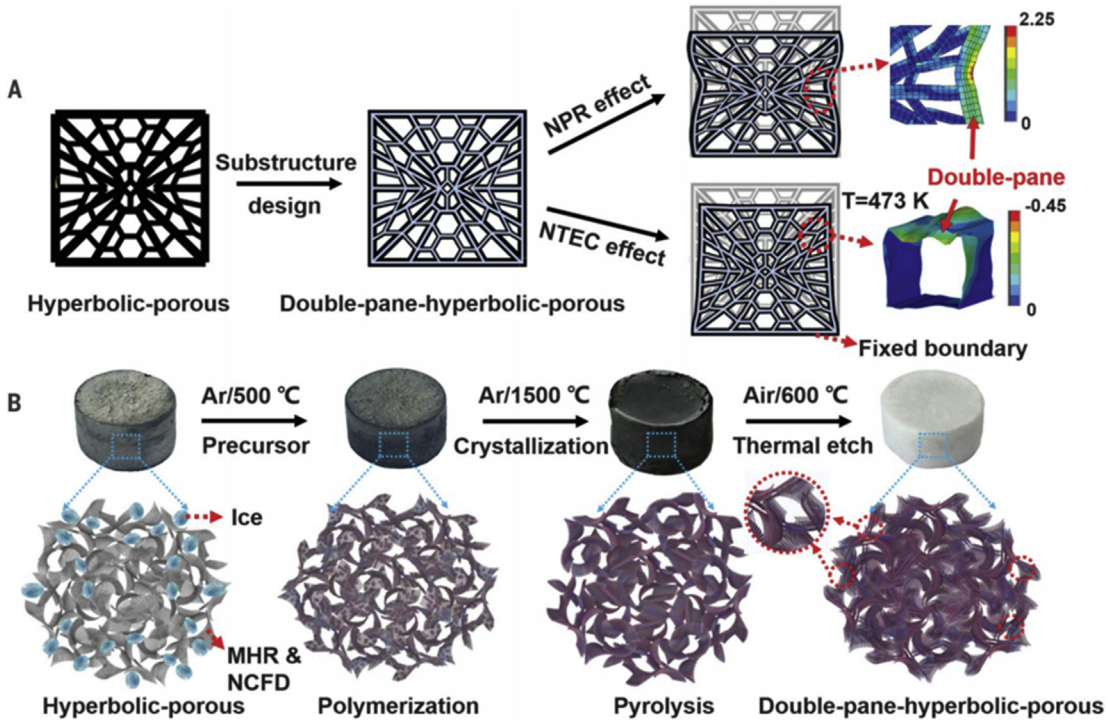

Fig. 9. Structure design and fabrication of ceramic aerogel metamaterials. (a) Schematic representation of the metastructure design of ceramic aerogels. The units of the colored scale bars are as follows: kilopascals for the NPR and percentage (with strain zoomed by 30 times) for the NTEC values. (b) Scheme of the chemical vapor deposition synthesis process of double-paned hyperbolic ceramic aerogels. NPR, negative Poisson's ratio; NTEC, negative temperature expansion coefficient. Reprinted with permission from Ref. [101]. Copyright © 2019.

technological applications, paved the way to the application of BN-based nanocomposites in the green energy, electrochemistry, and environment fields (discussed in the next section). However, studies on BN nanocomposites are still limited; mainly due to the high chemical stability of BN materials that prevent immediate reactions/modifications.

3. Applications

As BN nanocomposites are used to enhance the matrix strength and toughness, the obtained materials combine the beneficial properties of the different components. In the next sections, the most important applications of nanostructured BN and BN-based nanocomposites are reviewed, particularly in the energy, environment, and health fields.

3.1. Energy applications

3.1.1. Thermal conductivity

As BN possesses extraordinary thermal properties, much research has focused on the development of novel nanocomposites using BN as reinforcing nanofiller [102–105]. Indeed, single-layer h-BN has a theoretical thermal conductivity of ~ 1,700–2,000 W m^{-1} K^{-1}, therefore BN addition as nanofillers in different matrices can improve the nanocomposite thermal conductivity [23,106]. In nanocomposites, thermal conductivity can be enhanced by reducing the interfacial thermal resistance between nanofillers and polymer or ceramic matrices [103,107]. It is well known that thermal conductivity depends on the polymer matrix and the filler loads.

A study in which polymer/BN nanocomposites were prepared using epoxy resins and PVA as matrices reported different results in function of the used matrix. Epoxy/BN nanocomposites showed higher thermal diffusion than PVA/BN films. Indeed, epoxy resin is structurally more compatible with BNNSs, leading to reduced thermal transport. However, PVA/BN films offer better thermal conductivities at lower BN loads than epoxy/BN composites [44]. This study stimulated more research on PVA as polymer matrix. For example, Zhang et al. [108] prepared h-BN/PVA composites by vacuum filtration followed by PVA wetting. During the wetting step, some h-BN fillers diffuse through the polymer and form heat conductions paths. Diffusion reduces the polymer infiltration times and increases the nanocomposite thermal conductivity because of the creation of heat conduction paths (Fig. 10). The obtained h-BN/PVA nanocomposites reached a maximum thermal conductivity value of 8.44 W m^{-1} K^{-1} when h-BN was dispersed in the in-plane direction.

3.1.2. Photovoltaic/solar cells

Nanocomposites contribute to the multifunctionality and efficiency of solar cells, either as protective and photoactive layers, or as solar panel surfaces [25]. Graphene-on-silicon (Gr/Si) Schottky junction solar cells are cheap and ease to fabricate compared with the traditional Si solar cells, but their efficiency is still low. Introducing few-layered h-BN between graphene and n-Si can enhance the performance of Gr/Si Schottky junction solar cells. h-BN acts as an effective electron-blocking/hole-transporting layer by suppressing interface recombination [109].

Recently, perovskites have emerged as promising materials for solar cells because of their high absorption coefficients and

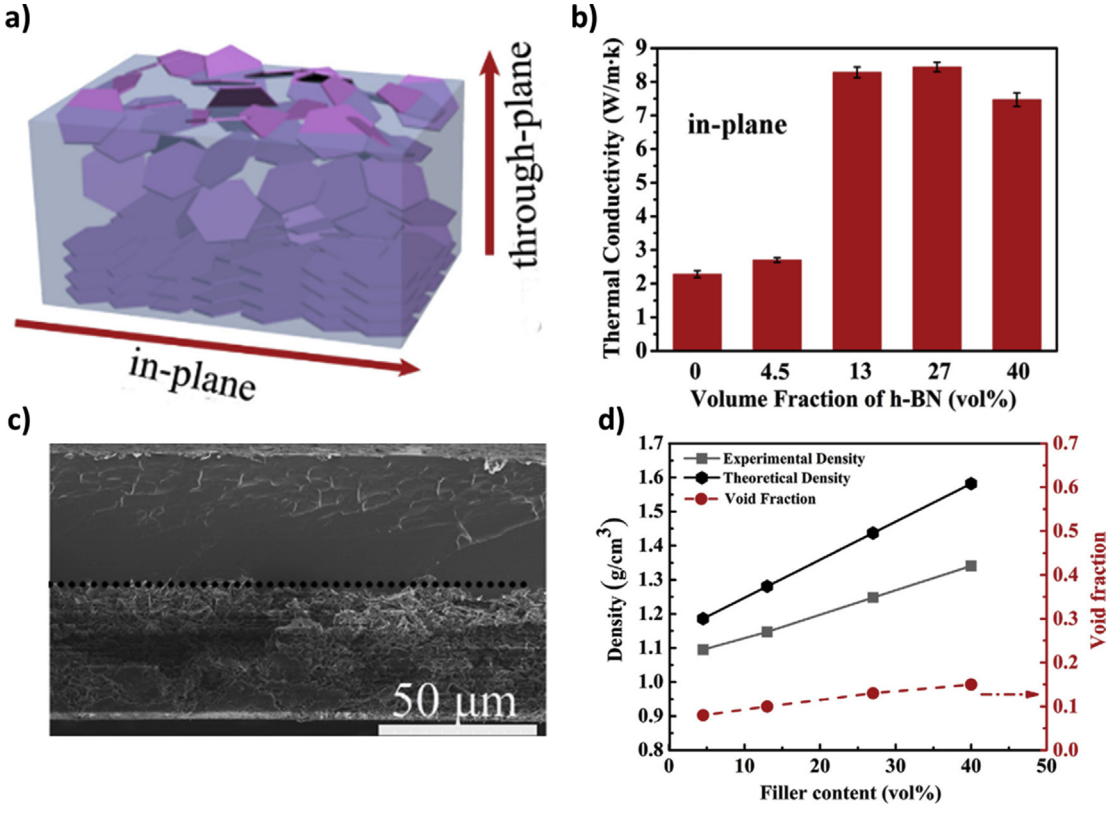

Fig. 10. (a) Schematic representation of filler distribution in the composite with the maximum thermal conductivity. (b) In-plane thermal conductivities of the h-BN/PVA composites in function of the h-BN volume fraction. (c) Scanning electron microscopy images of the side and front of a h-BN/PVA composite at 27 vol% loading. (d) Experimental density, theoretical density, and void fraction in function of the h-BN volume fraction. Reprinted with permission from Ref. [108]. Copyright © 2017, Elsevier Ltd.

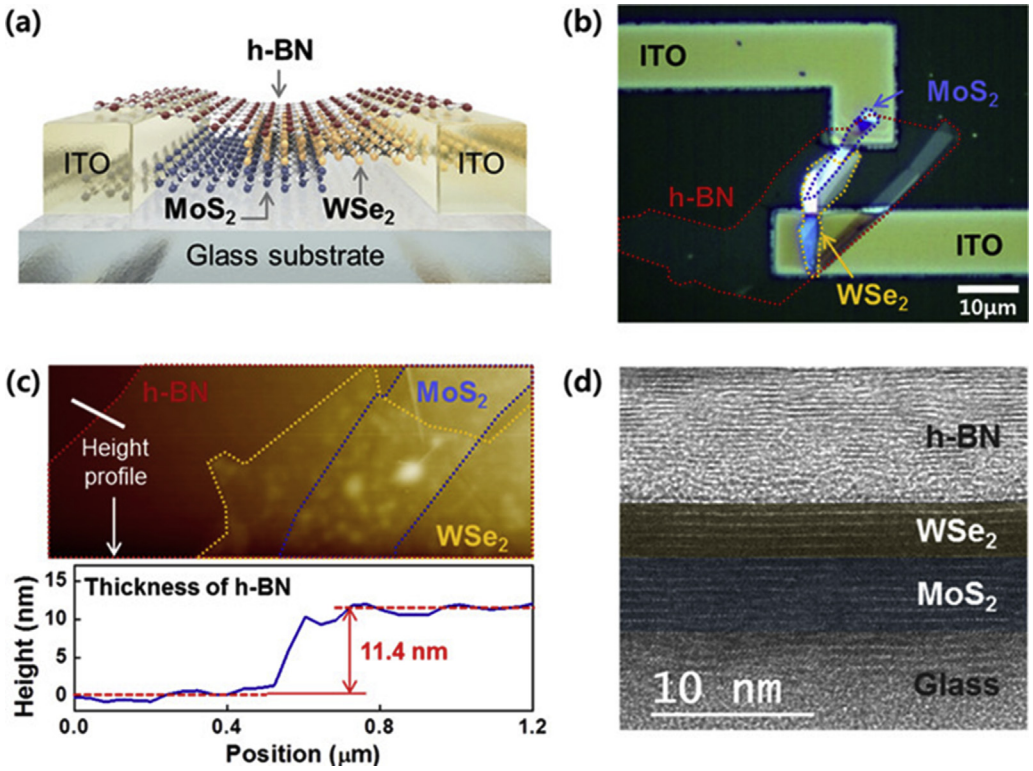

Fig. 11. (a) Schema showing the device used in the study by Cho et al. ITO, indium-tin oxide. (b) Optical microscopy image of the real device with each element. (c) Atomic force microscopy (AFM) image of the MoS_2/WSe_2/h-BN heterostructures (top) and the height profile of h-BN extracted from the AFM image (bottom). (d) False-color high-resolution transmission electron microscopy image showing the heterostructure cross-section. Reprinted with permission from Ref. [113]. Copyright © 2019, American Chemical Society

processability at low temperature [110]. The main drawback is their poor environmental stability [111] that can be improved by encapsulating the perovskites using h-BN materials. Seitz et al. [112] evaluated double-sided encapsulation with h-BN (h-BN/perovskite/h-BN) to provide long-term stability to phenethylammonium lead iodide 2D perovskites.

The structure of h-BN consists of stacked atomic layers held together by weak van der Waals interactions that allow forming van der Waals heterostructures with other 2D materials. Following this principle and by taking advantage of h-BN insulating behavior and inertness, heterojunction solar cells have been developed. Cho et al. [113] prepared MoS_2/WSe_2 heterojunction solar cells with h-BN passivation layer using a polydimethylsiloxane (PDMS)-mediated deterministic transfer process. The power conversion efficiency of their h-BN/MoS_2/WSe_2 heterojunction solar cells (Fig. 11) was improved by ~74% compared with unmodified h-BN material. This improvement is due to the reduced recombination rate at the junction and surface of the semiconductor regions.

3.1.3. Hydrogen storage and production

H_2 is an attractive renewable energy resource, but its generation and storage for practical applications are still challenging [114].

It has been demonstrated that low-dimension BN nanophase materials exhibit high H_2 uptake capacity because of stronger interactions with the heteropolar B—N bonds and partial H_2 chemisorption [115,116]. Highly porous BN micro-belts have been synthesized using a one-step, template-free reaction between boric acid-melamine precursors and ammonia at moderate conditions. This material has high specific surface area (1,488 $m^2\ g^{-1}$). Moreover, H_2 sorption analysis demonstrated that BN microbelts display reversible H_2 uptake from 1.6 to 2.3 wt% at 77 K (Fig. 12) and at relatively low pressure (1 MPa) [10]. Salameh et al. [96] developed a mesoporous monolithic (3D) BN structure using a template-assisted PDC route. The BN monoliths have a mesoporous network with a specific surface area ranging from 584 to 728 $m^2\ g^{-1}$, and show gravimetric H_2 storage capacity up to 8.1%.

BN nanocomposites could be used also for H_2 production. Different methods have been developed to increase H_2 production using different sources, such as photocatalysis [117] or electrocatalysis [118,119]. Titanium dioxide (TiO_2) is the most widely used material for photocatalysis. Doping TiO_2 with other species enhances the separation of the electron/hole pair. Nada et al. [117] produced new nanofiber composites by incorporating BNNSs in the structure of gadolinium-doped TiO_2 ($Gd_x/Ti_{(1-x)}O_{(4-X)/2}$). They found that BN presence created new impurity levels and improved the exciton life times. The BN/$Gd_xTi_{(1-x)}O_{(4-x)/2}$ nanocomposites displayed outstanding H_2 production performances by water splitting under visible light (up to 192.6 ± 1.5 mmol/g). Zhao et al. [120] developed a novel non-metal catalyst to produce H_2 by water splitting via h-BNNS band gap modification by chemical vapor deposition-mediated doping with sulfur atoms. The photocatalytic H_2 production efficiency was ~1,348.5 μmol $h^{-1}\ g^{-1}$, a value higher than what obtained with common visible light photocatalysts (S and g-C_3N_4).

Core-shell nanocomposites in which the inner metal core is encapsulated by porous materials have been developed as heterogeneous catalysts for H_2 production [121]. Liu et al. [122] fabricated cobalt-BN (Co@BN) core shell nanostructures through a one-step thermal treatment. The H_2 production efficiency of the as-prepared Co@BN nanocomposites was ~13.8 mmol $h^{-1}\ g^{-1}$.

Other H_2 production methods are based on thermolysis. Thermolysis of the chemical hydride does not require a noble metal catalyst and is relatively free of ammonia poisoning [123]. For example, Jin et al. [124] designed a hydrogen evolution reactor and

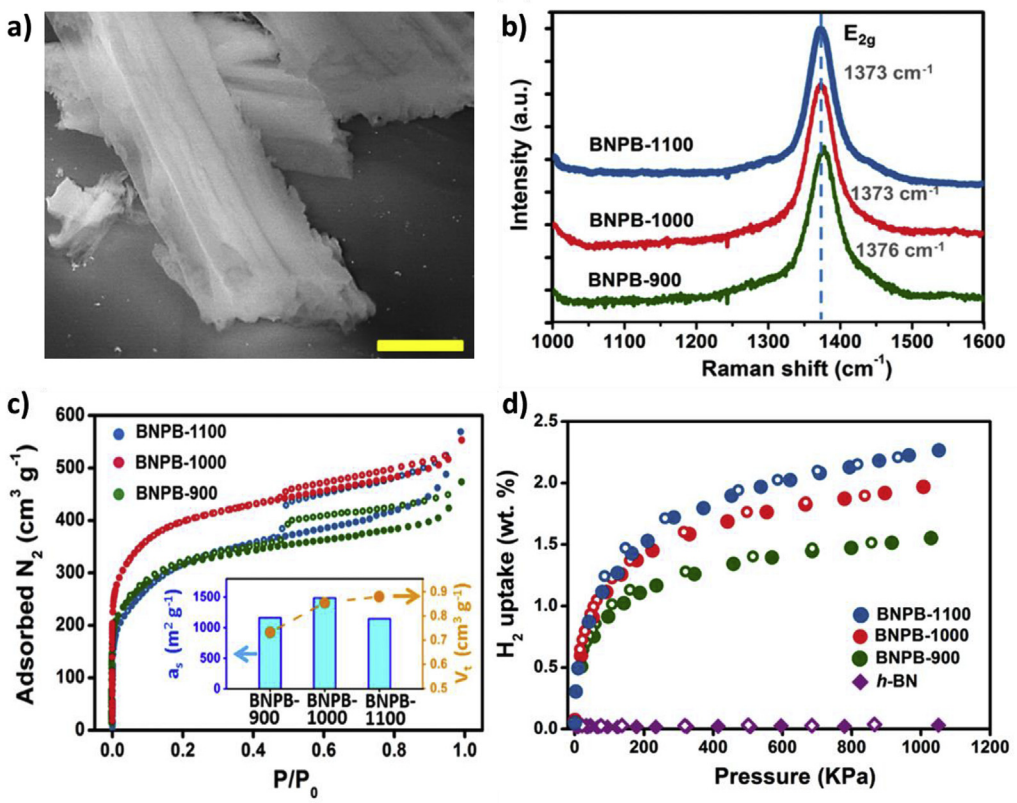

Fig. 12. (a) Tilted view of isolated porous structures, revealing a clear belt-shaped morphology; scale bar: 1 μm. (b) Raman spectra of BN porous microbelts prepared at different temperatures (900, 1,000, and 1,100°C). (c) Nitrogen adsorption–desorption isotherms of BN porous microbelts prepared at different temperatures (900, 1,000, and 1,100 °C). The inset in (c) shows the summary of the BET surface areas (a_s) and total pore volumes (Vt) for the obtained samples. (d) H_2 adsorption–desorption isotherms at 77 K and 1 MPa of BN porous microbelts. Reprinted with permission from Ref. [10]. Copyright © 2013, American Chemical Society.

hydrogen fuel composite to thermally decompose ammonia borane (AB) in the presence of silicon dioxide (SiO_2) nanoparticles to produce H_2. AB dehydrogenation reaction by the SiO_2 nanocatalyst composite produces H_2 with yields >12% and in less than 1 min.

3.1.4. Electrochemical applications

Rechargeable metal-ion batteries are a solution to the energy crisis related to the fossil fuel negative impact on the environment and civilization. However, the production of electrodes for such batteries is quite challenging. PDCs are an interesting choice for use in electrochemical devices [58]. Idrees et al. and Wan et al. [125,126] worked on PDC-based nanocomposites as stable electrodes for Li-ion batteries (LIB) for electrochemical applications. The combination of PDCs with other nanomaterials, such as carbon nanotubes [127,128], graphite [129], and BN [130], leads to structural modifications of their properties that are very useful for potential applications in LIB and supercapacitors. David et al. [130] showed that the integration of exfoliated BNNSs in SiCN significantly increases the charge capacity of free-standing SiCN-based LIB electrodes. Singh et al. [131] investigated how Li^+ insertion capacity could be increased by modifying SiOC ceramics with various BN nanotube (BNNT) loads. BNNTs presence in the composite affected the free carbon phase within the SiOC matrix. The higher ordering of the graphitic planes resulted in increased surface area of the SiOC-BNNT paper composite, thus influencing the electrochemical performance. Moreover, high BNNT load reduced the electroactive property of the resulting electrode. Conversely, SiOC loaded with 0.5 wt% BNNT showed higher capacitance when tested as electrode material for symmetric supercapacitors. Therefore, the composite may be used as a flexible electrode material for electrochemical energy storage devices, such as LIB and supercapacitors.

3.2. Environment

BN is thermally and chemically stable and has good resistance to oxidation. Furthermore, BN hydrophobic nature can be exploited to produce non-wetting surfaces and filtration systems. Therefore, BN is very interesting for emerging environmental applications, such as water technologies.

3.2.1. Water technologies

Novel BN-based materials have been developed for water technologies, particularly water purification. Owing to their good adsorption properties, BNNTs are excellent candidates for the sorption of pollutants, such as oil and organic solvents from heavy industries, and for water purification [14,132,133]. For instance, nanostructured BNNTs have been produced after deposition of borazine on polycarbonate and polyacrylonitrile membranes using a two-step atomic layer deposition (ALD) approach. The conformal pre-ceramic polymer layer is grown at low temperature (80 °C) using trichloroborazine and hexamethyldisilazane as precursors, and then is converted into dense h-BN. The hydrophobic behavior and high lipophilicity of the obtained nanostructures are interesting for oil/water separation [134]. Weber et al. [18] prepared BNNTs with controllable properties by combining ALD-mediated BN deposition on a carbon nanofiber template and annealing steps at high temperature. The obtained BNNTs presented good mechanical and sorption properties (oil uptake up to 110 times their own weight in oil while repelling water), and thus are very attractive for depollution applications.

BN-based nanocomposites for water purification have been fabricated also using the templating method. Gonzalez Ortiz et al. [19] developed novel h-BNNS/PVA-based nanocomposites. They prepared porous membranes by casting the homogeneous h-BNNS/PVA dispersion onto a glass support, followed by coagulation in a water bath to eliminate the solvent and create the porous structure. Then, they tested the h-BNNS/PVA nanocomposite permeability to pure water and particle rejection (Fig. 13), and found pure water permeability values of ~2,000 L h^{-1} m^{-2} bar^{-1} and a rejection efficiency of ~76% for particles of approximately 0.1μm in size. Other approaches, such as modified interfacial polymerization reaction, were developed to fabricate thin film nanocomposites decorated with amine-functionalized BNNSs. Owing to the amine functionalities and electron-deficient B atoms at the nanocomposite edges, these BNNSs are highly hydrophilic and negatively charged, thus limiting fouling. Compared with control material, these amine-functionalized BNNSs displayed a 59% increase in water flux (tested by cross-flow filtration experiments at 6 bars for 1 h) and a 50% improvement in total fouling resistance (using 0.2 g L^{-1} sodium alginate or bovine serum albumin solutions at neutral pH), while showing long-term functional stability [135]. Furthermore, antibiotics, such as tetracycline hydrochloride (TCH), can be removed from water by filtration using BN-based nanocomposites as membranes. TCH rejection by the membrane was stable (above 85%) in different conditions (acidic, alkaline pH, and saline solution), and permeability reached 240 L h^{-1} m^{-2} bar^{-1} [136].

BN can be used also to enhance TiO_2 photocatalytic activity for the treatment of pollutants in water. Nasr et al. [137] prepared new photocatalytic composite BNNS/TiO_2 nanofibers by electrospinning with different BNNS loads and evaluated their effect on the photocatalytic degradation of dyes under UV light. They found that BNNS addition increases the lattice strain in TiO_2 and reduces the recombination of charge carriers. The photocatalytic degradation of methyl orange using BNNS/TiO_2 nanofiber composites was four times higher than with free BNNS nanofibers. Addition of silver nanoparticles improved the antibacterial activity of such nanocomposites [138]. BNNS/TiO_2 nanocomposites have been also tested to remove other contaminants, such as ibuprofen, by photocatalytic oxidation. BNNS addition improved the light absorbance and reduced the electron/hole pair recombination. Moreover, the nanocomposite photocatalytic oxidation rate increased with higher BNNS loads [139].

3.2.2. Gas separation

Gas separation technologies are important in chemical industries because they are clean technologies with low energy requirements and high transport selectivity [140,141]. Nanocomposites fabricated from polymeric materials are extensively studied because they present some advantages, particularly light weight, high process flexibility, and low cost [142]. However, these materials display low gas permeation/separation properties. The polymer material permeability and selectivity can be improved by incorporating inorganic particles (e.g. 2D materials) in the polymer matrix [143–145]. Some theoretic calculations demonstrated h-BN potential applications for gas separation, for example, H_2/CH_4. Specifically, h-BN shows excellent H_2/CH_4 selectivity

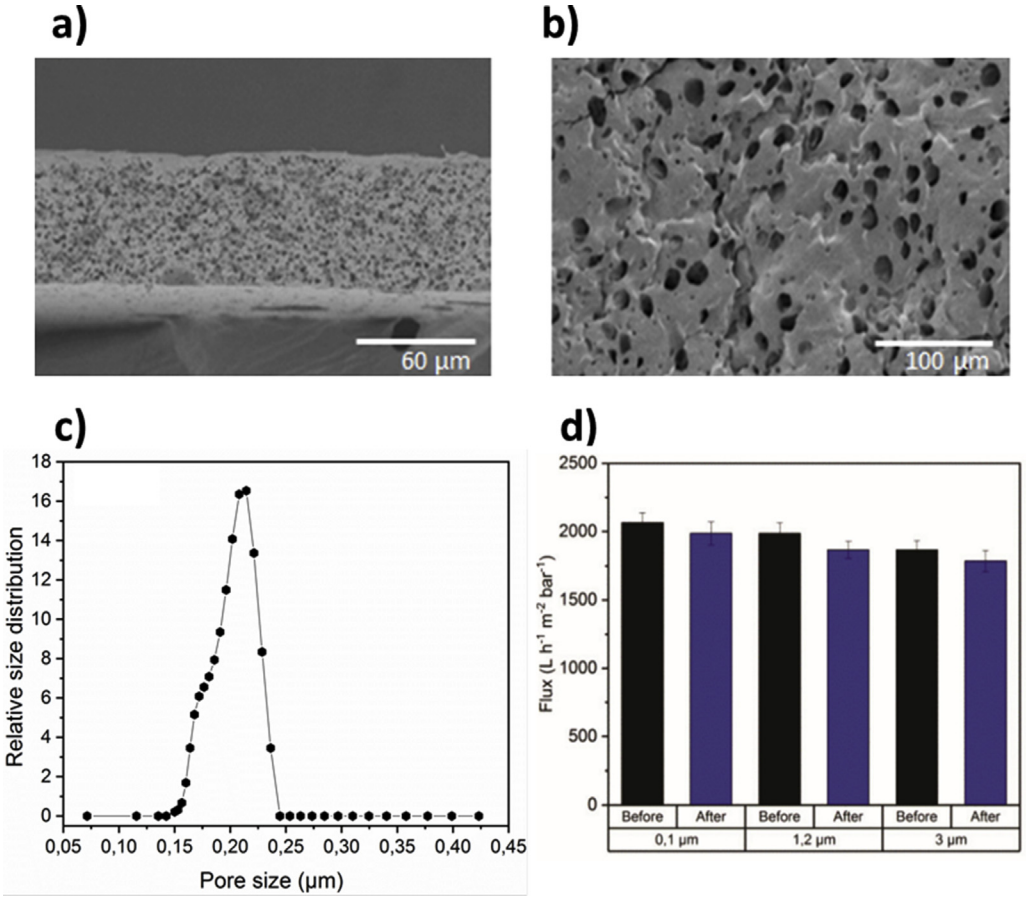

Fig. 13. Scanning electron microscopy photographs of the h-BNNS/PVA membrane nanocomposite: (a) cross-section and (b) surface. (c) Relative pore size distribution of the h-BNNS/PVA membrane, and (d) Corresponding fluxes of the h-BNNS/PVA membrane before and after the particle rejection tests. Reproduced with permission from Ref. [19].

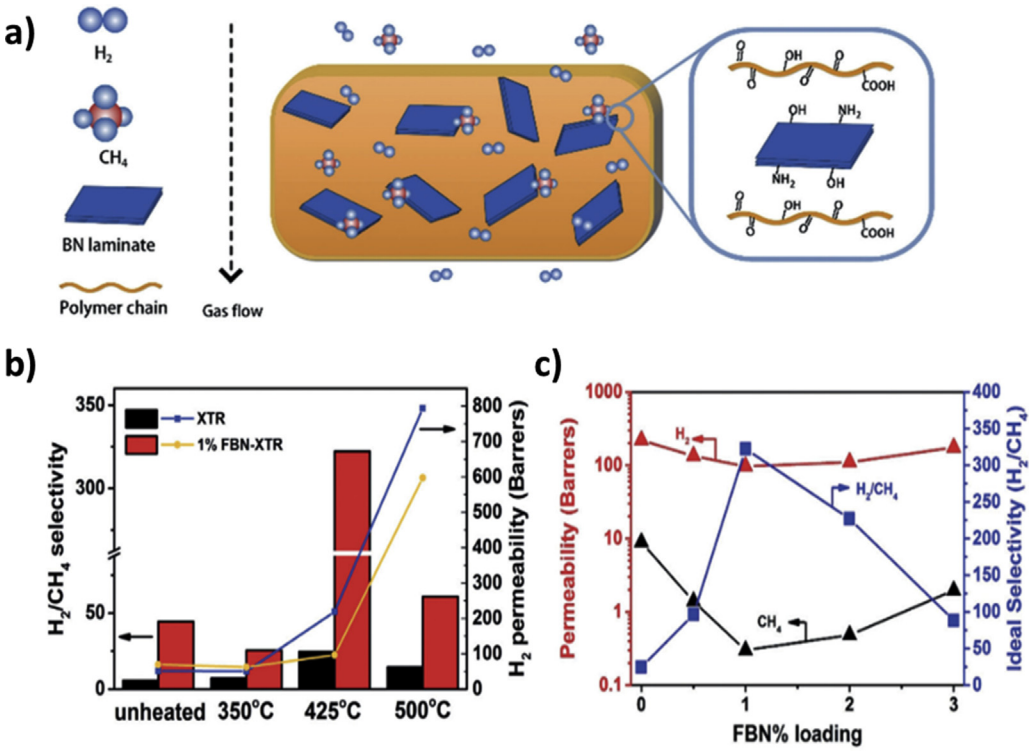

Fig. 14. (a) Schematic illustration of the FBN-XTR membrane structure and selective gas permeation through the membrane. (b) H_2 permeability and H_2/CH_4 selectivity of 1 wt% FBN-XTR and pure XTR membranes prepared at different thermal rearrangement temperatures. (c) Gas permeability and selectivity of membranes with different FBN loads, for the H_2/CH_4 pair at 258°C and 1 bar. Reprinted with permission from Ref. [147]. Copyright © 2018, Wiley-VCH Verlag GmbH & Co. KGaA, Weinheim.

($>10^5$ at room temperature) and low adsorption energies (0.1 eV more or less) for both H_2 and CH_4 on monolayer membranes [146]. h-BN has been used as nanofiller to improve the transport properties of polymer membranes, thanks to the specific adsorption effect of its functional groups. Functionalized BN nanosheets (FBN) have been used as fillers to tailor the gas transport and mechanical properties of thermally rearranged polyimide (XTR), thus producing an FBN-XTR nanocomposite (Fig. 14). FBN-XTR membranes were used for H_2 separation, with excellent H_2/CH_4 separation performance, higher than those of state-of-the-art membranes [147]. Kamble et al. [16] incorporated h-BN (0.35, 0.45, and 0.55 wt %) into a polyvinylidene fluoride (PVDF) matrix to fabricate homogeneous h-BN/PVDF nanocomposites by phase inversion. They demonstrated that h-BN incorporation improved the thermal and mechanical properties and also the gas (CO_2 and CH_4) permeability of the composite membranes. h-BN/PVDF (0.55 wt %) nanocomposites displayed permeabilities of 4.30559×10^5 and 3.19250×10^5 Barrer for CO_2 and CH_4, respectively. These studies pave the way to the development of new h-BN–based nanocomposites for gas separation technologies.

3.3. Health

3.3.1. Drug delivery

BN nanocomposites can be used also as drug delivery vectors. Indeed, due to its stability, flexibility, size and shape, low toxicity, and biodegradability, BN can be considered an ideal nanocarrier candidate. Nanoparticles should be small enough to travel in the blood vessels and penetrate into tissues, and large enough to avoid endothelial fenestrations. BN can be synthesized in different sizes that allow optimizing drug loading and delivery [148]. Duverger et al. [149] used density functional theory, time-dependent density functional theory, and molecular dynamic simulation methods to study the behavior of doxorubicin hydrochloride (DOX), an anticancer drug, loaded on BN oxide nanosheets (BNO-NS). This theoretical study showed that DOX molecules do not alter BNO-NS optical properties in aqueous media due to π–π and covalent interactions. Moreover, BNO-NS nanocarriers can stabilize DOX molecules on the cellular membrane, unlike isolated DOX molecules that randomly move without any interaction with the cell membrane. The same anticancer drug model was used to study the behavior of a targeted anticancer drug delivery system based on folate-conjugated BN nanospheres. Folic acid (FA) was successfully grafted onto BN nanospheres by esterification. The results showed that the nanosphere complexes are stable, as indicated by the absence of changes in particle size and polydispersity index in 5 days. Furthermore, DOX-releasing profile from the FA–BN nanospheres showed that it is pH-dependent and increases at lower pH [150]. Feng et al. improved the drug loading capacity of BN nanospheres by functionalization with folate-conjugated mesoporous silica (MS) (BNMS-FA). BNMS with core–shell structure was fabricated in two steps. First, tetraethylorthosilicate was hydrolyzed in the presence of cetyltrimethyl ammonium bromide to improve the dispersity. Then, FA was covalently grafted to BNMS complexes by amide reaction. Analysis of DOX release from BNMS-FA showed a sustained release pattern at low pH values. The *in-vitro* antitumor effect was also studied using BN nanospheres/DOX and BNMS/DOX complexes. BNMS/DOX complexes showed stronger effects because of the better DOX internalization mediated by the FA receptor (Fig. 15). These results suggest that BN nanospheres could be used for therapeutic applications, such as boron neutron capture [151]. Owing to its unique properties, including hierarchical porosity and high specific surface area, h-BN is suitable for drug delivery.

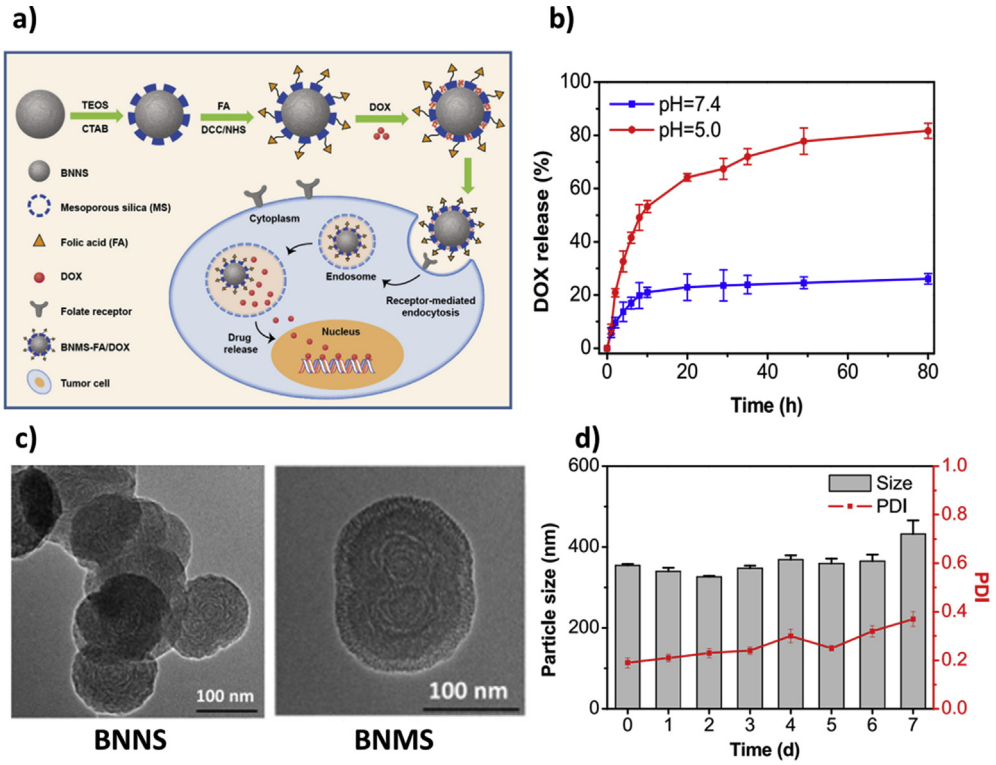

Fig. 15. (a) Schematic illustration of the preparation and application of folate-conjugated BNMS complexes for DOX targeted delivery. (b) pH-dependent DOX release from BNMS-FA/DOX complexes over time. (c) Transmission electron microscopy images of BN nanospheres and BNMS complexes. (d) Long-term stability of BNMS-FA (particle size and PDI) in phosphate-buffered saline at room temperature. PDI, polydispersity index. Reprinted with permission from Ref. [151]. Copyright © 2018, Elsevier Ltd.

3.3.2. Sensors

The development of new sensing devices (e.g. wearable biomedical electronic devices) and sensing functionalities (e.g. detection of species by fluorescence or colorimetric methods) has rapidly increased in the last years. Consequently, the design and production of functional nanocomposite materials with suitable physicochemical properties for fabricating sensors have become an important research field [152].

For the development of new sensing functionalities, BNNS with nanosized copper sulfide (CuS) dispersed on their surface (BNNS@CuS) were synthesized using an easy solvothermal approach. The authors used this sensing material for the visual detection of total cholesterol in human serum and they showed that BNNS@CuS devices display high selectivity toward cholesterol (linear range of 10–100 μM and a detection limit of 2.9 μM) [153]. As this approach is cheap, reliable, and effective, it paves the way to the development of novel sensing methods that exploit BN-based nanocomposite materials. Luo et al. synthesized h-BN whiskers using the polymeric precursor method, boric acid and melamine. Analysis of h-BN whisker performance as nitrite sensor using cyclic voltammetry and differential pulse voltammetry showed the appearance of a peak corresponding to nitrite oxidation and increased peak currents for NO_2 oxidation reactions. These results can be explained by the high porosity, large surface area, and high energy adsorption sites of h-BN whiskers [154].

Concerning novel sensing devices, Kim et al. [155] developed a transparent and flexible piezoelectric sensor (TFPS) system to detect the human body physical motion energy. The power device was synthesized using the sol-gel method and BNNS dispersed in PDMS. The produced TFPS using BN/PDMS nanocomposites was self-powered, transparent, flexible, and biocompatible (Fig. 16). The device can sense body movements and can generate electrical energy from such movements (e.g. folding and unfolding of joints) and from mechanical push force.

3.3.3. Tissue engineering

BNNSs can be used as reinforcement in nanocomposite or scaffold materials for tissue engineering and regenerative medicine because of their ability to enhance their mechanical and thermal properties without interfering with the polymer properties. Nagarajan et al. [156] synthesized gelatin/h-BNNS bio-nanocomposites by electrospinning and then crosslinked the nanocomposites to increase their stability in aqueous media. Exfoliated h-BN strengthened the electrospun gelatin fibers that were stable in phosphate-buffered saline. Viability assays using human osteosarcoma cells showed that h-BN does not influence cell attachment or proliferation, while increasing the nanocomposite mechanical properties. Furthermore, electrospun h-BNNS/gelatin mats are highly bioactive because of the formation of densely packed hydroxyapatite layers during mineralization in simulated body fluid. Three-dimensional nanostructured h-BN interconnected with boron trioxide (B_2O_3) (3D h-BN/B_2O_3) have been prepared by spark plasma sintering. The density (1.6–1.9 g/cm^3) and surface area (0.97–14.5 m^2/g) of the composite structure were significantly increased. Analysis of mouse calvaria osteoblast cell viability and proliferation on these materials, in view of a possible use as implant substitutes, showed no significant toxicity at different concentrations (from 1 to 100 μg/mL). Therefore, 3D h-BN/B_2O_3 nanocomposites are good candidates for bone implants because they are mechanically stable and promote cell viability and proliferation [157].

Another promising emerging technology in the field of tissue engineering is 3D printing because it allows fabricating many different artificial scaffolds to be used in tissue regeneration, cancer treatment, or the creation of artificial organs. Belaid et al. [158]

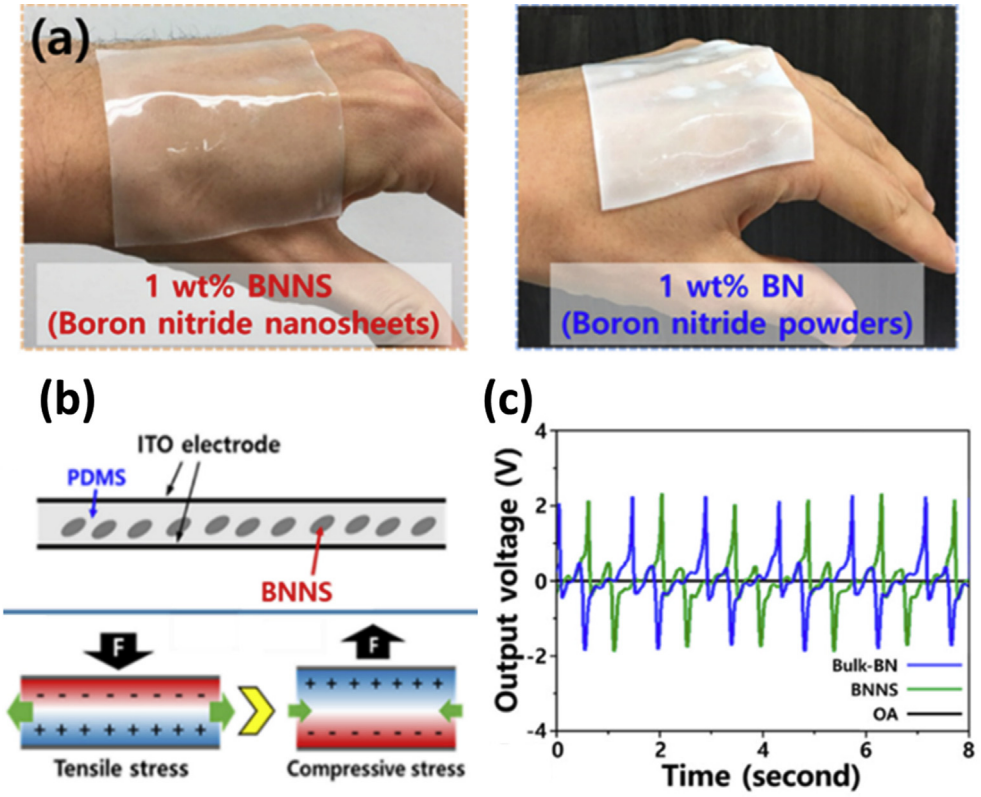

Fig. 16. (a) Comparison of the transparency of BNNS and bulk BN in PDMS-based composite devices attached to a human hand. (b) Schematic illustration of the working mechanism of the as-designed TFPS. (c) Open-circuit output voltage signals of BNNS, bulk-BN, and OA samples in PDMS-based composite devices under mechanical vibration (1.5 Hz). OA, oleylamine. Reprinted with permission from Ref. [155]. Copyright © 2018, Elsevier Ltd.

fabricated a 3D multifunctional PLA scaffold reinforced with h-BNNS (PLA/h-BNNS) with a well interconnected porous structure by fused deposition modeling (FDM)—based 3D printing. Analysis of the attachment and proliferation of osteoblast cells (MG-63 and MC3T3) showed that PLA/h-BNNS biomimetic scaffolds are non-toxic and promote the attachment, proliferation, and differentiation of cells with osteogenic potential. Although h-BN—based scaffolds are very interesting supports for bone regeneration (Fig. 17), research on 3D-printed h-BN scaffold applications for tissue engineering is still in its early days.

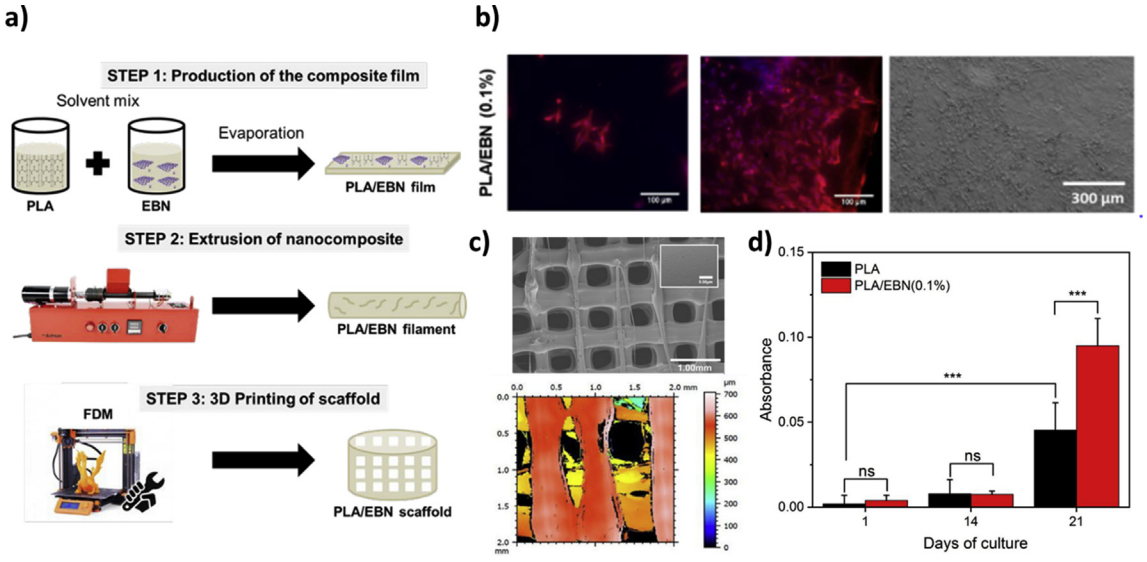

Fig. 17. (a) Schematic representation of the different steps of scaffold generation. (b) Attachment of MG-63 cells on PLA-based nanocomposites was analyzed by immunofluorescence staining of actin (red), DNA (blue), and by scanning electron microscopy. (c) Scanning electron microscopy images and topography of FDM-based 3D-printed PLA/exfoliated BN (EBN) scaffolds. (d) Mineralization evaluated by Alizarin Red-S staining of MG-63 cells cultured on PLA and PLA/EBN nanocomposite scaffolds at different time points after switching to differentiation medium. Reproduced with permission from Ref. [158]. Copyright © 2020, American Chemical Society

Besides these BN applications in the health field, h-BN possesses also antibacterial and anticancer effects [159–161]. For instance, a vertically aligned composite material using BN and a low-density polyethylene (LDPE) polymer (BN-LDPE composite) displays a highly structured morphology with BN oriented in the extrusion flow direction. Its antibacterial activity was evaluated by culturing some common pathogens on these composites and by counting the colony forming units. The results suggest that in this composite, BN kills the bacteria directly rather than by inhibiting bacterial attachment [162]. For anticancer effects, hollow BN nanospheres were synthesized by chemical vapor deposition using trimethoxyborane and ammonia as precursors. The fabricated hollow BN spheres showed controlled crystallinity and solubility and could guide the release of boron by adjusting the post-treatment temperature. Two prostate cancer cells line, androgen-sensitive LNCap and androgen-independent DU-145 cells, were used to evaluate the effects of hollow BN spheres on apoptosis, necrosis, and proliferation *in vitro* [163]. These results suggest that BN nanospheres might be interesting candidate therapeutic agents to inhibit tumor recurrence in patients with prostate cancer.

4. Conclusions and outlook

This review summarized the current research on BN-based nanomaterials in terms of synthesis methods and prospective applications. First, the different synthesis methods to produce polymer nanocomposites reinforced with BN were described (e.g. melt intercalation/blending, in-situ polymerization intercalation, template synthesis, and solvent mixing). Moreover, the use of preceramic polymers as BN precursors facilitates processing before nanocomposite generation (dip-coating, spin-coating, casting, warm or cold pressing). Porosity can be controlled with templating and non-templating strategies. Although great progress has been made in the synthesis of polymer and ceramic nanomaterials, novel and effective synthesis approaches using harmless solvents and with limited energy consumption should be investigated. Furthermore, more efforts have to be made toward the development of strategies to produce nanostructured materials with well-controlled size, shape, composition, and spatial arrangement. In addition, it would be interesting to study the scalability of these strategies to produce materials at the industrial scale because currently, most of the methods used to produce these nanomaterials are at the laboratory scale.

Here, we outlined the trends for the synthesis of novel BN-based nanocomposites. Additional interface engineering via chemical modification or by other methods to enhance the interaction between matrices and nanofillers, such as binding, will be the next important objective. The development of novel strategies to produce BN-based materials with controlled architectures is highly desired. Liquid-phase atomic layer deposition (LALD) could be a simple solution-phase deposition processes to produce these materials. LALD principle is similar to that of the classical ALD process, but a solution of precursors is used instead of gas precursors, and purging is not required. This technique ensures the layer-by-layer growth of materials with the same precision as gas-phase ALD. Furthermore, the subsequent injections of stoichiometric quantities of precursor will avoid any unwanted reaction in solution. This approach should allow producing well-ordered BN-based nanocomposites, by controlling the deposition rate, thickness, and roughness of nanocomposites. LALD could be used for preparing polymer- and ceramic-based BN nanocomposites. The PDC route is considered the best approach to synthesize new BN liquid preceramic precursors adapted to LALD.

The development of printable materials also is a good alternative strategy to produce nanostructured, polymeric- and ceramic-based BN nanocomposites. Thanks to their unique formability and much lower melting point compared with ceramics, polymers are at a much more advanced stage of development. Very few additive manufacturing (AM) techniques are suitable for ceramic materials, and most of them use ceramic powders as feedstock. Owing to the high melting point of ceramics, powder consolidation to a dense material is a big challenge, and residual porosity is very hard to avoid. One interesting solution would be to couple the PDC route with AM where the preceramic polymer can be molecularly and structurally engineered to be directly printed at the polymeric state before its ceramic conversion. Various types of 3D printers using different AM approaches to produce scaffolds are commercially available, such as the stereolithographic printer that uses a resin containing photopolymers to produce a matrix. BN nanoparticles can be added to enhance their properties. Another interesting printer approach is selective laser sintering that uses high-power CO_2 lasers to fuse particles together and can produce ceramic- and polymer-based scaffolds.

BN-based nanocomposites materials are interesting because of the excellent properties that BN brings to these materials, such as chemical stability, mechanical strength, resistance to oxidation, thermal conductivity, and heat and electrical insulation. Much research is focusing on the possible applications of such BN-based nanomaterials in the energy, environment, and health fields. One of the remaining challenges is to carefully control the nanofiller dispersion and orientation in the matrices, a crucial point to optimize the nanocomposite performances. The development of cell-compatible BNNT and BN nanoplatelet nanocomposites with improved mechanical properties opens new avenues for *in vitro* and *in vivo* safety and efficacy studies in view of bone tissue engineering and self-healing applications. Despite the significant progress in the development of BN-based nanocomposites, their practical applications are still challenging and many obstacles must be overcome, such as their durability and recovery. From the point of view of sustainability, more research is needed on novel polymer-based nanocomposites from clean, sustainable, and renewable energy sources. The new devices for sensing applications and novel nanocomposites for water purification are promising outcomes of the research on BN-based materials. Moreover, as BN networks exhibit low thermal resistance and interfacial heat scattering, BN-based nanocomposites could be used as high-performance heat spreaders in next-generation thermal management systems. Improvements in the field of photovoltaic cells are also expected, such as easy manufacturing of high-performance devices, reduced processing costs, and simple implementation of flexible and transparent cell modules. BN-based nanocomposites could be good candidates to meet such expectations.

Declaration of competing interest

The authors declare that they have no known competing financial interests or personal relationships that could have appeared to influence the work reported in this paper.

References

[1] M. Nasrollahzadeh, Z. Issaabadi, M. Sajjadi, S.M. Sajadi, M. Atarod, Types of nanostructures, in: Mahmoud Nasrollahzadeh, S. Mohammad Sajadi, Mohaddeseh Sajjadi, Zahra Issaabadi, Monireh Atarod (Eds.), Interface Science and Technology, vol. 28, Elsevier Ltd., 2019, pp. 29–80, https://doi.org/10.1016/B978-0-12-813586-0.00002-X.

[2] M. Emanet, Ö. Sen, I.Ç. Taşkin, M. Çulha, Synthesis, functionalization, and bioapplications of two-dimensional boron nitride nanomaterials, Front. Bioeng. Biotechnol. 7 (2019) 363, https://doi.org/10.3389/fbioe.2019.00363.

[3] J. Wang, F. Ma, M. Sun, Graphene, hexagonal boron nitride, and their heterostructures: properties and applications, RSC Adv. 7 (2017) 16801–16822, https://doi.org/10.1039/C7RA00260B.

[4] H. Zeng, C. Zhi, Z. Zhang, X. Wei, X. Wang, W. Guo, Y. Bando, D. Golberg, 'White graphenes': boron nitride nanoribbons via boron nitride nanotube unwrapping, Nano Lett. 10 (12) (2010) 5049–5055, https://doi.org/10.1021/nl103251m.

[5] D. Gonzalez Ortiz, C. Pochat-Bohatier, J. Cambedouzou, M. Bechelany, P. Miele, Exfoliation of hexagonal boron nitride (h-BN) in liquide phase by ion intercalation, Nanomaterials 8 (9) (2018) 716, https://doi.org/10.3390/nano8090716.

[6] A.M. Patki, R.K. Goyal, High performance polyetherketone-hexagonal boron nitride nanocomposites for electronic applications, J. Mater. Sci. Mater. Electron. 30 (2019) 3899–3908, https://doi.org/10.1007/s10854-019-00675-9.

[7] Q. Li, L. Chen, M.R. Gadinski, S. Zhang, H.H. Li, E. Iagodkine, A. Haque, L.Q. Chen, T.N. Jackson, Q. Wang, Flexible hig-temperature dielectric materials from polymer nanocomposites, Nature 523 (2015) 576–579, https://doi.org/10.1038/nature14647.

[8] H. Oh, J. Kim, Fabrication of polymethyl methacrylate composites with silanized boron nitride by in-situ polymerization for high thermal conductivity, Compos. Sci. Technol. 172 (2019) 153–162, https://doi.org/10.1016/j.compscitech.2019.01.021.

[9] V. Thangaraj, J. Bussiere, J.M. Janot, M. Bechelany, M. Jaber, S. Subramanian, P. Miele, S. Balme, Fluorescence quenching of sulforhodamine dye over graphene oxide and boron nitride nanosheets, Eur. J. Inorg. Chem. 2016 (13–14) (2016) 2125–2130, https://doi.org/10.1002/ejic.201501153.

[10] Q. Weng, X. Wang, C. Zhi, Y. Bando, D. Golberg, Boron nitride porous microbelts for hydrogen storage, ACS Nano 7 (2) (2013) 1558–1565, https://doi.org/10.1021/nn305320v.

[11] R. Naresh Muthu, S. Rajashabala, R. Kannan, Hexagonal boron nitride (h-BN) nanoparticles decorated multi-walled carbon nanotubes (MWCNT) for hydrogen storage, Renew. Energy 85 (2016) 387–394, https://doi.org/10.1016/j.renene.2015.06.056.

[12] B. Farshid, G. Lalwani, M. Shir Mohammadi, J. Simonsen, B. Sitharaman, Boron nitride nanotubes and nanoplatelets as reinforcing agents of polymeric matrices for bone tissue engineering, J. Biomed. Mater. Res. B Appl. Biomater. 105 (2) (2017) 406–419, https://doi.org/10.1002/jbm.b.33565.

[13] M. Jedrzejczak-Silicka, M. Trukawka, M. Dudziak, K. Piotrowska, E. Mijowska, Hexagonal boron nitride functionalized with Au nanoparticles—properties and potential biological applications, Nanomaterials 8 (8) (2018) 605, https://doi.org/10.3390/nano8080605.

[14] S. Yu, X. Wang, H. Pang, R. Zhang, W. Song, D. Fu, T. Hayat, X. Wang, Boron nitride-based materials for the removal of pollutants from aqueous solutions: a review, Chem. Eng. J. 333 (2018) 343–360, https://doi.org/10.1016/j.cej.2017.09.163.

[15] C. Chen, J. Wang, D. Liu, C. Yang, Y. Liu, R.S. Ruoff, W. Lei, Functionalized boron nitride membranes with ultrafast solvent transport performance for molecular separation, Nat. Commun. 9 (2018) 1902, https://doi.org/10.1038/s41467-018-04294-6.

[16] A.R. Kamble, C.M. Patel, Z.V.P. Murthy, Effects of inorganic additive of two-dimensional hexagonal boron nitride on the gas separation/permeation for PVDF-derived membranes, Separ. Sci. Technol. 54 (9) (2019) 1489–1501, https://doi.org/10.1080/01496395.2019.1577451.

[17] M. Weber, B. Koonkaew, S. Balme, I. Utke, F. Picaud, I. Iatsunskyi, E. Coy, P. Miele, M. Bechelany, Boron nitride nanoporous membranes with high surface charge by atomic layer deposition, ACS Appl. Mater. Interfaces 9 (19) (2017) 16669–16678, https://doi.org/10.1021/acsami.7b02883.

[18] M. Weber, I. Iatsunskyi, E. Coy, P. Miele, M. Bechelany, Novel and facile route for the synthesis of tunable boron nitride nanotubes combining atomic layer deposition and annealing processes for water purification, Adv. Mater. Interfaces 5 (16) (2018) 1800056, https://doi.org/10.1002/admi.201800056.

[19] D. Gonzalez-Ortiz, C. Pochat-Bohatier, S. Gassara, J. Cambedouzou, M. Bechelany, P. Miele, Development of novel h-BNNS/PVA porous membranes via Pickering emulsion templating, Green Chem. 20 (2018) 4319–4329, https://doi.org/10.1039/C8GC01983E.

[20] A. Pakdel, C. Zhi, Y. Bando, D. Golberg, Low-dimensional boron nitride nanomaterials, Mater. Today (2012), https://doi.org/10.1016/S1369-7021(12)70116-5.

[21] S. Bernard, P. Miele, Nanostructured and architectured boron nitride from boron, nitrogen and hydrogen-containing molecular and polymeric precursors, Mater. Today 17 (9) (2014) 443–450, https://doi.org/10.1016/j.mattod.2014.07.006.

[22] S. Bernard, C. Salameh, P. Miele, Boron nitride ceramics from molecular precursors: synthesis, properties and applications, Dalton Trans. 45 (2016) 861–873, https://doi.org/10.1039/C5DT03633J.

[23] Q. Weng, X. Wang, X. Wang, Y. Bando, D. Golberg, Functionalized hexagonal boron nitride nanomaterials: emerging properties and applications, Chem. Soc. Rev. 45 (2016) 3989–4012, https://doi.org/10.1039/C5CS00869G.

[24] S. Yu, X. Wang, H. Pang, R. Zhang, W. Song, D. Fu, T. Hayat, X. Wang, Boron nitride-based materials for the removal of pollutants from aqueous solutions: a review, Chem. Eng. J. (2018), https://doi.org/10.1016/j.cej.2017.09.163.

[25] K. Müller, E. Bugnicourt, M. Latorre, M. Jorda, Y. Etchegoyen Sanz, J.M. Lagaron, O. Misbauer, A. Bianchin, S. Kankin, U. Bölz, G. Pérez, M. Jesdinszki, M. Lindner, Z. Scheuerer, S. Castello, M. Schmid, Review on the processing and properties of polymer nanocomposites and nanocoatings and their applications in the packaging, automotive and solar energy fields, Nanomaterials 7 (2017) 74, https://doi.org/10.3390/nano7040074.

[26] S.C. Tjong, Structural and mechanical properties of polymer nanocomposites, Mater. Sci. Eng. R: Rep. 53 (3–4) (2006) 73–197, https://doi.org/10.1016/j.mser.2006.06.001.

[27] J. Biscarat, M. Bechelany, C. Pochat-Bohatier, P. Miele, Graphene-like BN/gelatin nanobiocomposites for gas barrier applications, Nanoscale 7 (2015) 613–618, https://doi.org/10.1039/C4NR05268D.

[28] G. Alva, Y. Lin, G. Fang, Thermal and electrical characterization of polymer/ceramic composites with polyvinyl butyral matrix, Mater. Chem. Phys. 205 (2018) 401–415, https://doi.org/10.1016/j.matchemphys.2017.11.046.

[29] X. Dai, C. Hou, Z. Xu, Y. Yang, G. Zhu, P. Chen, Z. Huang, L. Yan, Entropic effects in polymer nanocomposites, Entropy 21 (2) (2019), 186, https://doi.org/10.3390/e21020186.

[30] A. Dantas de Oliveira, C. Augusto Gonçalves Beatrice, Polymer nanocomposites with different types of nanofiller. Nanocomposites - Recent Evol., 2019, https://doi.org/10.5772/intechopen.81329.

[31] A. Usuki, M. Kawasumi, Y. Kojima, A. Okada, T. Kurauchi, O. Kamigaito, Swelling behavior of montmorillonite cation exchanged for ω -amino acids by e-caprolactam, J. Mater. Res. 8 (5) (1993) 1174–1178, https://doi.org/10.1557/JMR.1993.1174.

[32] Y. Kojima, A. Usuki, M. Kawasumi, A. Okada, T. Kurauchi, O. Kamigaito, One-pot synthesis of nylon 6-clay hybrid, J. Mater. Res. 31 (7) (1993) 1755–1758, https://doi.org/10.1002/pola.1993.080310714.

[33] I.U. Unalan, E. Marcuzzo, S. Farris, Nanocomposite films and coatings using inorganic nanobuilding blocks (NBB): current applications and future opportunities in the food packaging sector, RSC Adv. 4 (2014) 29393–29428, https://doi.org/10.1039/c4ra01778a.

[34] C. Emrah, C. Koçyigit, S. Cakir, A. Durmus, M.V. Kahraman, Preparation and characterization of thermally conductive thermoplastic polyurethane/h-BN nanocomposites, Polym. Compos. 35 (3) (2014) 530–538, https://doi.org/10.1002/pc.22692.

[35] M. Öner, A.A. Çöl, C. Pochat-Bohatier, M. Bechelany, Effect of incorporation of boron nitride nanoparticles on the oxygen barrier and thermal properties of poly(3-hydroxybutyrate-*co*-hydroxyvalerate), RSC Adv. 6 (2016) 90973–90981, https://doi.org/10.1039/C6RA19198C.

[36] Z. Wang, Q. Li, Z. Chen, J. Liu, T. Liu, H. Li, S. Zheng, Enhanced comprehensive properties of nylon-6 nanocomposites by aniline-modified boron nitride nanosheets, Ind. Eng. Chem. Res. 57 (32) (2018) 11005–11013, https://doi.org/10.1021/acs.iecr.8b02005.

[37] X. Huang, S. Wang, M. Zhu, K. Yang, P. Jiang, Y. Bando, D. Goldberg, C. Zhi, Thermally conductive, electrically insulating and melt-processable polystyrene/boron nitride nanocomposites prepared by in situ reversible addition fragmentation chain transfer polymerization, Nanotechnology 26 (1) (2015), 015705, https://doi.org/10.1088/0957-4484/26/1/015705.

[38] X. Yang, Y. Guo, X. Luo, N. Zheng, T. Ma, J. Tan, C. Li, Q. Zhang, J. Gu, Self-healing, recoverable epoxy elastomers and their composites with desirable thermal conductivities by incorporating BN fillers via in-situ polymerization, Compos. Sci. Technol. 164 (2018) 59–64, https://doi.org/10.1016/j.compscitech.2018.05.038.

[39] R. Wang, H. Cheng, Y. Gong, F. Wang, X. Ding, R. Hu, X. Zhang, J. He, X. Tian, Highly thermally conductive polymer composite originated from assembly of boron nitride at an oil-water interface, ACS Appl. Mater. Interfaces 11 (45) (2019) 42818–42826, https://doi.org/10.1021/acsami.9b15259.

[40] Y. Liu, J. Goebl, Y. Yin, Templated synthesis of nanostructured materials, Chem. Soc. Rev. 42 (2013) 2610–2653, https://doi.org/10.1039/C2CS35369E.

[41] X. Zeng, Y. Yao, Z. Gong, F. Wang, R. Sun, J. Xu, C.P. Wong, Ice-templated assembly strategy to construct 3D boron nitride nanosheet networks in polymer composites for thermal conductivity improvement, Small 11 (46) (2015) 6205–6213, https://doi.org/10.1002/smll.201502173.

[42] D. Gonzalez Ortiz, C. Pochat-Bohatier, J. Cambedouzou, M. Bechelany, P. Miele, Current trends in pickering emulsions: particle morphology and applications, Engineering 6 (4) (2020) 468–482, https://doi.org/10.1016/j.eng.2019.08.017.

[43] R.K. Nayak, K.K. Mahato, B.C. Ray, Processing of polymer-based nanocomposites, in: Pramendra K. Bajpai, Inderdeep Singh (Eds.), Reinforced Polymer Composites: Processing, Characterization and Post Life Cycle Assessment, 2019, pp. 55–75, https://doi.org/10.1002/9783527820979.ch4.

[44] W.L. Song, L. Cao, A. Anderson, M.J. Meziani, A.J. Farr, Y.P. Sun, Polymer/boron nitride nanocomposite materials for superior thermal transport performance, Angew. Chem. Int. Ed. 51 (26) (2012) 6498–6501, https://doi.org/10.1002/anie.201201689.

[45] T. Morishita, H. Okamoto, Facile exfoliation and noncovalent superacid functionalization of boron nitride nanosheets and their use for highly thermally conductive and electrically insulating polymer nanocomposites, ACS Appl. Mater. Interfaces 8 (40) (2016) 27064–27073, https://doi.org/10.1021/acsami.6b08404.

[46] X. Zhang, H. Chen, H. Ye, A. Liu, L. Xu, Enhanced interfacial polarization in poly(vinylidene fluoride- chlorotrifluoroethylene) nanocomposite with parallel boron nitride nanosheets, Nanotechnology 31 (2020) 165703, https://doi.org/10.1088/1361-6528/ab69b4.

[47] L. Tammaro, V. Vittoria, V. Bugatti, Dispersion of modified layered double hydroxides in Poly(ethylene terephthalate) by High Energy Ball Milling for food packaging applications, Eur. Polym. J. 52 (2014) 172–180, https://doi.org/10.1016/j.eurpolymj.2014.01.001.

[48] K. Niihara, New design concept of structural ceramics, J. Ceram. Soc. Japan 99 (1991) 974–982, https://doi.org/10.2109/jcersj.99.974.

[49] Y. Sakka, D.D. Bidinger, I.A. Aksay, Processing of silicon carbide-mullite-alumina nanocomposites, J. Am. Ceram. Soc. 78 (2) (1995) 479–486, https://doi.org/10.1111/j.1151-2916.1995.tb08827.x.

[50] L. Carroll, M. Sternitzke, B. Derby, Silicon carbide particle size effects in alumina-based nanocomposites, Acta Mater. 44 (11) (1996) 4543–4552, https://doi.org/10.1016/1359-6454(96)00074-2.

[51] S. Guo, R. Sivakumar, H. Kitazawa, Y. Kagawa, Electrical properties of silica-based nanocomposites with multiwall carbon nanotubes, J. Am. Ceram. Soc. 90 (5) (2007) 1667–1670, https://doi.org/10.1111/j.1551-2916.2007.01636.x.

[52] N. Sharma, S.N. Alam, B.C. Ray, S. Yadav, K. Biswas, Wear behavior of silica and alumina-based nanocomposites reinforced with multi walled carbon nanotubes and graphene nanoplatelets, Wear 418–419 (2019) 290–304, https://doi.org/10.1016/j.wear.2018.10.008.

[53] H. Takada, A. Nakahira, S. Ueda, K. Niihara, H. Ohnishi, Improvement of mechanical properties of natural mullite/SiC nanocomposites, J. Jpn. Soc. Powder Powder Metall. 38 (1991) 348–351, https://doi.org/10.2497/jjspm.38.348.

[54] A.W. Weimer, R.K. Bordia, Processing and properties of nanophase SiC/Si3N4 composites, Compos.: Part B 30 (7) (1999) 647–655, https://doi.org/10.1016/S1359-8368(99)00039-6.

[55] M. Kong, W. Zhao, L. Wei, G. Li, Investigations on the microstructure and hardening mechanism of TiN/Si3N4 nanocomposite coatings, J. Phys. D Appl. Phys. 40 (9) (2007), 2858, https://doi.org/10.1088/0022-3727/40/9/029.

[56] S. Bajwa, W.M. Rainforth, W.E. Lee, Sliding wear behaviour of SiC–Al2O3 nanocomposites, Wear 259 (1–6) (2005) 553–561, https://doi.org/10.1016/j.wear.2005.02.027.

[57] E. Ionescu, H.J. Kleebe, R. Riedel, Silicon-containing polymer-derived ceramic nanocomposites (PDC-NCs): preparative approaches and properties, Chem. Soc. Rev. 41 (2012) 5032–5052, https://doi.org/10.1039/C2CS15319J.

[58] P. Colombo, G. Mera, R. Riedel, G.D. Sorarù, Polymer-derived ceramics: 40 Years of research and innovation in advanced ceramics, J. Am. Ceram. Soc. 93 (7) (2010) 1805–1837, https://doi.org/10.1111/j.1551-2916.2010.03876.x.

[59] S. Yajima, J. Hayashi, M. Omori, Continuous silicon carbide fiber of high tensile strength, Chem. Lett. 4 (9) (1975) 931–934, https://doi.org/10.1246/cl.1975.931.

[60] S. Yajima, J. Hayashi, M. Omori, K. Okamura, Development of a silicon carbide fibre with high tensile strength, Nature 261 (1976) 683–685, https://doi.org/10.1038/261683a0.

[61] M. Günthner, T. Kraus, A. Dierdorf, D. Decker, W. Krenkel, G. Motz, Advanced coatings on the basis of Si(C)N precursors for protection of steel against oxidation, J. Eur. Ceram. Soc. 29 (10) (2009) 2061–2068, https://doi.org/10.1016/j.jeurceramsoc.2008.11.013.

[62] G.D. Sorarù, F. Dalcanale, R. Campostrini, A. Gaston, Y. Blum, S. Carturan, P.R. Aravind, Novel polysiloxane and polycarbosilane aerogels via hydrosilylation of preceramic polymers, J. Mater. Chem. 22 (2012) 7676–7680, https://doi.org/10.1039/C2JM00020B.

[63] C. Salameh, A. Bruma, S. Malo, U.B. Demirci, P. Miele, S. Bernard, Monodisperse platinum nanoparticles supported on highly ordered mesoporous silicon nitride nanoblocks: superior catalytic activity for hydrogen generation from sodium borohydride, RSC Adv. 5 (2015) 58943–58951, https://doi.org/10.1039/C5RA05901A.

[64] M. Schmidt, C. Durif, E. Diz Acosta, C. Salameh, H. Plaisantin, P. Miele, R. Backov, R. Machado, C. Gervais, J.G. Alauzun, G. Chollon, S. Bernard, Molecular-level processing of Si-(B)-C materials with tailored nano/microstructures, Chem. Eur J. 23 (67) (2017) 17103–17117, https://doi.org/10.1002/chem.201703674.

[65] R.M. Prasad, Y. Iwamoto, R. Riedel, A. Gurlo, Multilayer amorphous-Si-B-C-N/γ-Al2O3/α- Al2O3 membranes for hydrogen purification, Adv. Eng. Mater. 12 (6) (2010) 522–528, https://doi.org/10.1002/adem.201000095.

[66] F. Cheng, S.M. Kelly, N.A. Young, C.N. Hope, K. Beverley, M.G. Francesconi, S. Clark, J.S. Bradley, F. Lefebvre, Preparation of mesoporous Pd/Si3N4 nanocomposites as heterogeneous catalysts via three different chemical routes, Chem. Mater. 18 (25) (2006) 5996–6005, https://doi.org/10.1021/cm061106h.

[67] G. Mera, P. Kroll, I. Ponomarev, J. Chen, K. Mojita, M. Liesegang, E. Ionescu, A. Navrotsky, Metal-catalyst-free access to multiwalled carbon nanotubes/silica nanocomposites (MWCNT/SiO2) from a single-source precursor, Dalton Trans. 48 (2019) 11018–11033, https://doi.org/10.1039/C9DT01783F.

[68] X. Wang, G. Mera, K. Morita, E. Ionescu, Synthesis of polymer-derived graphene/silicon nitride-based nanocomposites with tunable dielectric properties, J. Ceram. Soc. Japan 124 (10) (2016) 981–988, https://doi.org/10.2109/jcersj2.16089.

[69] P. Greil, Active-filler-controlled pyrolysis of preceramic polymers, J. Am. Ceram. Soc. 78 (4) (1995) 835–848, https://doi.org/10.1111/j.1151-2916.1995.tb08404.x.

[70] K.A. Youngdhal, M.L. Hoppe, R.M. Laine, J.A. Rahn, J.F. Harrod, Synthesis of inorganic polymers as glass precursors and for other uses: pre-ceramic block or graft copolymers as potential precursors to composite materials, Appl. Organomet. Chem. 7 (8) (1993) 647–654, https://doi.org/10.1002/aoc.590070808.

[71] D. Seyferth, H. Lang, C.A. Sobon, J. Borm, H.J. Tracy, N. Bryson, Chemical modification of preceramic polymers: their reactions with transition metal complexes and transition metal powders, J. Inorg. Organomet. Polym. 2 (1992) 59–77, https://doi.org/10.1007/BF00696536.

[72] T. Ishikawa, H. Yamaoka, Y. Harada, T. Fujii, T. Nagasawa, A general process for in situ formation of functional surface layers on ceramics, Nature 416 (2002) 64–67, https://doi.org/10.1038/416064a.

[73] S. Veprek, A. Niederhofer, K. Moto, T. Bolom, H.D. Männling, P. Nesladek, G. Dollinger, A. Bergmaier, Composition, nanostructure and origin of the ultrahardness in nc-TiN/a-Si3N4/a- and nc-TiSi2 nanocomposites with Hv = 80 to ≥105 GPa, Surf. Coating. Technol. 133–134 (2000) 152–159, https://doi.org/10.1016/S0257-8972(00)00957-9.

[74] M.C. Bechelany, V. Proust, A. Lale, P. Miele, S. Malo, C. Gervais, S. Bernard, Nanocomposites through the chemistry of single-source precursors: understanding the role of chemistry behind the design of monolith-type nanostructured titanium nitride/silicon nitride, Chem. Eur J. 23 (4) (2017) 832–845, https://doi.org/10.1002/chem.201603661.

[75] R. Riedel, L. Toma, C. Fasel, G. Miehe, Polymer-derived mullite–SiC-based nanocomposites, J. Eur. Ceram. Soc. 29 (14) (2009) 3079–3090, https://doi.org/10.1016/j.jeurceramsoc.2009.05.016.

[76] E. Ionescu, C. Linck, C. Fasel, M. Müller, H.J. Kleebe, R. Riedel, Polymer-derived SiOC/ZrO2 ceramic nanocomposites with excellent high-temperature stability, J. Am. Ceram. Soc. 93 (1) (2010) 241–250, https://doi.org/10.1111/j.1551-2916.2009.03395.x.

[77] H.Y. Jin, H. Xu, G.J. Qiao, J.Q. Gao, Z.H. Jin, Study of machinable silicon carbide-boron nitride ceramic composites, Mater. Sci. Eng. A 483–484 (2008) 214–217, https://doi.org/10.1016/j.msea.2006.12.165.

[78] X. Wang, G. Qiao, Z. Jin, Fabrication of machinable silicon carbide-boron nitride ceramic nanocomposites, J. Am. Ceram. Soc. 87 (4) (2004) 565–570, https://doi.org/10.1111/j.1551-2916.2004.00565.x.

[79] T. Kusunose, T. Sekino, Y.-H. Choa, K. Niihara, Machinability of silicon nitride/boron nitride nanocomposites, J. Am. Ceram. Soc. 85 (11) (2002) 2689–2695, https://doi.org/10.1111/j.1151-2916.2002.tb00515.x.

[80] C. Doche, F. Guilhon, B. Bonnetot, F. Thevenot, H. Mongeot, Elaboration and characterization of Si3N4-BN composites from tris(methylamino)borane as a boron nitride precursor, J. Mater. Sci. Lett. 14 (1995) 847–850.

[81] Y. Li, G. Qiao, Z. Jin, Machinable Al2O3/BN composite ceramics with strong mechanical properties, Mater. Res. Bull. 37 (8) (2002) 1401–1409, https://doi.org/10.1016/S0025-5408(02)00786-9.

[82] T. Kusunose, Y.H. Kim, T. Sekino, T. Matsumoto, N. Tanaka, T. Nakayama, K. Nihara, Fabrication of Al_2O_3/BN nanocomposites by chemical processing and their mechanical properties, J. Mater. Res. 20 (1) (2005) 183–190, https://doi.org/10.1557/JMR.2005.0010.

[83] S.G. Prilliman, S.M. Clark, A.P. Alivisatos, P. Karvankova, S. Vepřek, Strain and deformation in ultra-hard nanocomposites nc-TiN/a-BN under hydrostatic pressure, Mater. Sci. Eng. A 437 (2) (2006) 379–387, https://doi.org/10.1016/j.msea.2006.07.126.

[84] R.F. Zhang, S.H. Sheng, S. Veprek, Stability of Ti-B-N solid solutions and the formation of nc-TiN/a-BN nanocomposites studied by combined ab initio and thermodynamic calculations, Acta Mater. 56 (16) (2008) 4440–4449, https://doi.org/10.1016/j.actamat.2008.04.066.

[85] A. Mège-Revil, P. Steyer, S. Cardinal, G. Thollet, C. Esnouf, P. Jacquot, B. Stauder, Correlation between thermal fatigue and thermomechanical properties during the oxidation of multilayered TiSiN nanocomposite coatings synthesized by a hybrid physical/chemical vapour deposition process, Thin Solid Films 518 (21) (2010) 5932–5937, https://doi.org/10.1016/j.tsf.2010.05.092.

[86] T. Wideman, L.G. Sneddon, Convenient procedures for the laboratory preparation of borazine, Inorg. Chem. 34 (4) (1995) 1002–1003, https://doi.org/10.1021/ic00108a039.

[87] L.G. Sneddon, T. Wideman, Method for Synthesis of Borazine, 1997. US patent 5612013 (1997), patent.

[88] S. Bernard, M. Bechelany, J. Li, P. Miele, W. Zhong, Precursors of Metal-loborazine Type, Process and Materials Obtained from Such Precursors, 2011. Patent n°: WO/2011/121225. (2011), patent.

[89] W. Zhong, Préparation de matériaux à base de nitrure de bore pour des applications 'énergie', PhD Thesis, Univ Montpellier, 2012.

[90] W. Zhong, S. Wang, J. Li, M.C. Bechelany, R. Ghisleni, F. Rossignol, C. Balan, T. Chartier, S. Bernard, P. Miele, Design of carbon fiber reinforced boron nitride matrix composites by vacuum-assisted polyborazylene transfer molding and pyrolysis, J. Eur. Ceram. Soc. 33 (15–16) (2013) 2979–2992, https://doi.org/10.1016/j.jeurceramsoc.2013.06.013.

[91] P. Dibandjo, L. Bois, F. Chassagneux, D. Cornu, J.M. Letoffe, B. Toury, F. Babonneau, P. Miele, Synthesis of boron nitride with ordered mesostructure, Adv. Mater. 17 (5) (2005) 571–574, https://doi.org/10.1002/adma.200401501.

[92] J.G. Alauzun, S. Ungureanu, N. Brun, S. Bernard, P. Miele, R. Backov, C. Sanchez, Novel monolith-type boron nitride hierarchical foams obtained through integrative chemistry, J. Mater. Chem. 21 (2011) 14025–14030, https://doi.org/10.1039/C1JM12751A.

[93] G. Moussa, C. Salameh, A. Bruma, S. Malo, U.B. Demirci, S. Bernard, P. Miele, Nanostructured boron nitride: from molecular design to hydrogen storage application, Inorganics 2 (3) (2014) 396–409, https://doi.org/10.3390/inorganics2030396.

[94] Q. Weng, X. Wang, X. Wang, Y. Bando, D. Golberg, Functionalized hexagonal boron nitride nanomaterials: emerging properties and applications, Chem. Soc. Rev. 45 (2016) 3989–4012, https://doi.org/10.1039/C5CS00869G.

[95] P. Dibandjo, L. Bois, F. Chassagneux, P. Miele, Thermal stability of mesoporous boron nitride templated with a cationic surfactant, J. Eur. Ceram. Soc. 27 (1) (2007) 313–317, https://doi.org/10.1016/j.jeurceramsoc.2006.04.178.
[96] C. Salameh, G. Moussa, A. Bruma, G. Fantozzi, S. Malo, P. Miele, U.B. Demirci, S. Bernard, et al., Robust 3D boron nitride nanoscaffolds for remarkable hydrogen storage capacity from ammonia borane, Energy Technol. 6 (3) (2018) 570–577, https://doi.org/10.1002/ente.201700618.
[97] P. Wu, W. Zhu, Y. Chao, J. Zhang, P. Zhang, H. Zhu, C. Li, Z. Chen, H. Li, S. Dai, A template-free solvent-mediated synthesis of high surface area boron nitride nanosheets for aerobic oxidative desulfurization, Chem. Commun. 52 (2016) 144–147, https://doi.org/10.1039/C5CC07830J.
[98] S. Bernard, P. Miele, Ordered mesoporous polymer-derived ceramics and their processing into hierarchically porous boron nitride and silicoboron carbonitride monoliths, New J. Chem. 38 (2014) 1923–1931, https://doi.org/10.1039/C3NJ01612A.
[99] A.C. Pierre, G.M. Pajonk, Chemistry of aerogels and their applications, Chem. Rev. 102 (11) (2002) 4243–4266, https://doi.org/10.1021/cr0101306.
[100] L.W. Hrubesh, R.W. Pekala, Thermal properties of organic and inorganic aerogels, J. Mater. Res. 9 (3) (1994) 731–738, https://doi.org/10.1557/JMR.1994.0731.
[101] X. Xu, Q. Zhang, M. Hao, Y. Hu, Z. Li, L. Peng, T. Wang, X. Ren, C. Wang, Z. Zhao, C. Wan, H. Fei, L. Wang, J. Zhu, H. Sun, W. Chen, T. Du, B. Deng, G.J. Cheng, I. Shakir, C. Dames, T.S. Fisher, X. Zhang, H. Li, Y. Huang, X. Duan, Double-negative-index ceramic aerogels for thermal superinsulation, Science 363 (6428) (2019) 723–727, https://doi.org/10.1126/science.aav7304.
[102] J. Hou, G. Li, L. Qin, M.E. Grami, Q. Zhang, N. Wang, X. Qu, Preparation and characterization of surface modified boron nitride epoxy composites with enhanced thermal conductivity, RSC Adv. 4 (2014) 44282–44290, https://doi.org/10.1039/C4RA07394K.
[103] Z. Lin, A. Mcnamara, Y. Liu, K. Moon, sik, C.P. Wong, Exfoliated hexagonal boron nitride-based polymer nanocomposite with enhanced thermal conductivity for electronic encapsulation, Compos. Sci. Technol. 90 (2014) 123–128, https://doi.org/10.1016/j.compscitech.2013.10.018.
[104] V. Guerra, C. Wan, T. McNally, Thermal conductivity of 2D nano-structured boron nitride (BN) and its composites with polymers, Prog. Mater. Sci. 100 (2019) 170–186, https://doi.org/10.1016/j.pmatsci.2018.10.002.
[105] D. Mishra, S. Mohapatra, A. Satapathy, A detailed investigation on thermal and micro-structural properties of hexagonal boron nitride composites, Mater. Today Proc. 5 (9(3)) (2018) 19747–19753, https://doi.org/10.1016/j.matpr.2018.06.337.
[106] T. Ouyang, Y. Chen, Y. Xie, K. Yang, Z. Bao, J. Zhong, Thermal transport in hexagonal boron nitride nanoribbons, Nanotechnology 21 (2010), 245701, https://doi.org/10.1088/0957-4484/21/24/245701.
[107] C. Zou, C. Zhang, B. Li, S. Wang, Z. Xie, Y. Song, Fabrication and properties of borazine derived boron nitride matrix wave-transparent composites reinforced by 2.5 dimensional fabric of Si-N-O fibers, Mater. Sci. Eng. A 620 (2015) 420–427, https://doi.org/10.1016/j.msea.2014.10.046.
[108] J. Zhang, X. Wang, C. Yu, Q. Li, Z. Li, C. Li, H. Lu, Q. Zhang, J. Zhao, M. Hu, Y. Yao, A facile method to prepare flexible boron nitride/poly(vinyl alcohol) composites with enhanced thermal conductivity, Compos. Sci. Technol. 149 (2017) 41–47, https://doi.org/10.1016/j.compscitech.2017.06.008.
[109] J.H. Meng, X. Liu, X.W. Zhang, Y. Zhang, H.L. Wang, Z.G. Yin, Y.Z. Zhang, H. Liu, J.B. You, H. Yan, Interface engineering for highly efficient graphene-on-silicon Schottky junction solar cells by introducing a hexagonal boron nitride interlayer, Nano Energy 28 (2016) 44–50, https://doi.org/10.1016/j.nanoen.2016.08.028.
[110] M.A. Green, A. Ho-Baillie, H.J. Snaith, The emergence of perovskite solar cells, Nat. Photon. 8 (2014) 506–514, https://doi.org/10.1038/nphoton.2014.134.
[111] S. Yang, W. Fu, Z. Zhang, H. Chen, C.Z. Li, Recent advances in perovskite solar cells: efficiency, stability and lead-free perovskite, J. Mater. Chem. A 5 (2017) 11462–11482, https://doi.org/10.1039/C7TA00366H.
[112] M. Seitz, P. Gant, A. Castellanos-Gomez, F. Prins, Long-term stabilization of two-dimensional perovskites by encapsulation with hexagonal boron nitride, Nanomaterials 9 (8) (2019), 1120, https://doi.org/10.3390/nano9081120.
[113] A.J. Cho, J.Y. Kwon, Hexagonal boron nitride for surface passivation of two-dimensional van der Waals heterojunction solar cells, ACS Appl. Mater. Interfaces 11 (43) (2019) 39765–39771, https://doi.org/10.1021/acsami.9b11219.
[114] H. Zhang, C.J. Tong, Y. Zhang, Y.N. Zhang, L.M. Liu, Porous BN for hydrogen generation and storage, J. Mater. Chem. A 3 (2015) 9632–9637, https://doi.org/10.1039/C5TA01052G.
[115] S.H. Lim, J. Luo, W. Ji, J. Lin, Synthesis of boron nitride nanotubes and its hydrogen uptake, Catal. Today 120 (3–4) (2007) 346–350, https://doi.org/10.1016/j.cattod.2006.09.016.
[116] A. Lale, S. Bernard, U.B. Demirci, Boron nitride for hydrogen storage, Chem.Plus.Chem 83 (10) (2018) 893–903, https://doi.org/10.1002/cplu.201800168.
[117] A.A. Nada, M.F. Bekheet, R. Viter, P. Miele, S. Roualdes, M. Bechelany, BN/GdxTi(1-x)O(4-x)/2 nanofibers for enhanced photocatalytic hydrogen production under visible light, Appl. Catal. B Environ. 251 (2019) 76–86, https://doi.org/10.1016/j.apcatb.2019.03.043.
[118] M. Weber, N. Tuleushova, J. Zgheib, C. Lamboux, I. Iatsunskyi, E. Coy, V. Flaud, S. Tingry, D. Cornu, P. Miele, M. Bechelany, Y. Holade, Enhanced electrocatalytic performance triggered by atomically bridged boron nitride between palladium nanoparticles and carbon fibers in gas-diffusion electrodes, Appl. Catal. B Environ. 257 (2019), 117917, https://doi.org/10.1016/j.apcatb.2019.117917.
[119] S. Kawrani, A.A. Nada, M.F. Beckheet, M. Boulos, R. Viter, S. Roualdes, P. Miele, D. Cornu, M. Bechelany, Enhancement of calcium copper titanium oxide photoelectrochemical performance using boron nitride nanosheets, Chem. Eng. J. 389 (2020), 124326, https://doi.org/10.1016/j.cej.2020.124326.
[120] G. Zhao, A. Wang, W. He, Y. Xing, X. Xu, 2D new nonmetal photocatalyst of sulfur-doped h-BN nanosheeets with high photocatalytic activity, Adv. Mater. Interfaces 6 (7) (2019), 1900062, https://doi.org/10.1002/admi.201900062.
[121] J. Liu, et al., Metal@semiconductor core-shell nanocrystals with atomically organized interfaces for efficient hot electron-mediated photocatalysis, Nano Energy 48 (2018) 44–52.
[122] Q. Liu, Q. Liu, Z. Li, C. Cheng, M. Song, C. Huang, Photocatalysis under shell: Co@BN core–shell composites for efficient EY-sensitized photocatalytic hydrogen evolution, Appl. Surf. Sci. 514 (2020), 146096, https://doi.org/10.1016/j.apsusc.2020.146096.
[123] J. Luo, X. Kang, C. Chen, J. Song, D. Luo, P. Wang, Rapidly releasing over 9 wt % of H2 from NH3BH3-Mg or NH3BH3-MgH2 composites around 85 °c, J. Phys. Chem. C 120 (33) (2016) 18386–18393, https://doi.org/10.1021/acs.jpcc.6b04230.
[124] J.H. Jin, S. Shin, J. Jung, N.F. Attia, Solid-phase hydrogen storage based on NH3BH3-SiO2 nanocomposite for thermolysis, J. Nanomater. (2019), 6126031, https://doi.org/10.1155/2019/6126031.
[125] M. Idrees, S. Batool, J. Kong, Q. Zhuang, H. Liu, Q. Shao, N. Lu, Y. Feng, E.K. Wujcik, T. Ding, R. Wei, Z. Guo, Polyborosilazane derived ceramics - nitrogen sulfur dual doped graphene nanocomposite anode for enhanced lithium ion batteries, Electrochim. Acta 296 (2019) 925–937, https://doi.org/10.1016/j.electacta.2018.11.088.
[126] J. Wan, A.K. Mukherjee, M.J. Gasch, Nanocomposites of Silicon Nitride, Silicon Carbide, and Boron Nitride, 2006. Patent 7077991 B2, US Patent.
[127] S. Sarkar, J. Zou, J. Liu, C. Xu, L. An, L. Zhai, Polymer-derived ceramic composite fibers with aligned pristine multiwalled carbon nanotubes, ACS Appl. Mater. Interfaces 2 (4) (2010) 1150–1156, https://doi.org/10.1021/am1000085.
[128] R. Bhandavat, G. Singh, Stable and efficient li-ion battery anodes prepared from polymer-derived silicon oxycarbide-carbon nanotube shell/core composites, J. Phys. Chem. C 117 (23) (2013) 11899–11905, https://doi.org/10.1021/jp310733b.
[129] M. Graczyk-Zajac, C. Fasel, R. Riedel, Polymer-derived-SiCN ceramic/graphite composite as anode material with enhanced rate capability for lithium ion batteries, J. Power Sources 196 (15) (2011) 6412–6418, https://doi.org/10.1016/j.jpowsour.2011.03.076.
[130] L. David, S. Bernard, C. Gervais, P. Miele, G. Singh, Facile synthesis and high rate capability of silicon carbonitride/boron nitride composite with a sheet-like morphology, J. Phys. Chem. C 119 (5) (2015) 2783–2791, https://doi.org/10.1021/jp508075x.
[131] M.A. Abass, A.A. Syed, C. Gervais, G. Singh, Synthesis and electrochemical performance of a polymer-derived silicon oxycarbide/boron nitride nanotube composite, RSC Adv. 7 (2017) 21576–21584, https://doi.org/10.1039/C7RA01545C.
[132] W. Lei, D. Portehault, D. Liu, S. Qin, Y. Chen, Porous boron nitride nanosheets for effective water cleaning, Nat. Commun. 4 (2013), 1777, https://doi.org/10.1038/ncomms2818.
[133] T. Li, L. Wang, K. Zhang, Y. Xu, X. Long, S. Gao, R. Li, Y. Yao, Freestanding boron nitride nanosheet films for ultrafast oil/water separation, Small 12 (36) (2016) 4960–4965, https://doi.org/10.1002/smll.201601298.
[134] W. Hao, C. Marichy, C. Journet, A. Brioude, A novel two-step ammonia-free atomic layer deposition approach for boron nitride, ChemNanoMat 3 (9) (2017) 656–663, https://doi.org/10.1002/cnma.201700148.
[135] S. Abdikheibari, W. Lei, L.F. Dumée, A.J. Barlow, K. Baskaran, Novel thin film nanocomposite membranes decorated with few-layered boron nitride nanosheets for simultaneously enhanced water flux and organic fouling resistance, Appl. Surf. Sci. 488 (2019) 565–577, https://doi.org/10.1016/j.apsusc.2019.05.217.
[136] G. Yang, D. Zhang, C. Wang, H. Liu, L. Qu, H. Li, A novel nanocomposite membrane combining bn nanosheets and go for effective removal of antibiotic in water, Nanomaterials 9 (3) (2019), 386, https://doi.org/10.3390/nano9030386.
[137] M. Nasr, R. Viter, C. Eid, R. Habchi, P. Miele, M. Bechelany, Enhanced photocatalytic performance of novel electrospun BN/TiO2 composite nanofibers, New J. Chem. 41 (2017) 81–89, https://doi.org/10.1039/C6NJ03088B.
[138] M. Nasr, L. Soussan, R. Viter, C. Eid, R. Habchi, P. Miele, M. Bechelany, High photodegradation and antibacterial activity of BN-Ag/TiO2 composite nanofibers under visible light, New J. Chem. 42 (2018) 1250–1259, https://doi.org/10.1039/C7NJ03183A.
[139] L. Lin, W. Jiang, M. Bechelany, M. Nasr, J. Jarvis, T. Schaub, R.R. Sapkota, P. Miele, H. Wang, P. Xu, Adsorption and photocatalytic oxidation of ibuprofen using nanocomposites of TiO2 nanofibers combined with BN nanosheets: degradation products and mechanisms, Chemosphere 220 (2019) 921–929, https://doi.org/10.1016/j.chemosphere.2018.12.184.
[140] G. Dong, H. Li, V. Chen, Challenges and opportunities for mixed-matrix membranes for gas separation, J. Mater. Chem. A 1 (2013) 4610–4630, https://doi.org/10.1039/C3TA00927K.

[141] D.F. Sanders, Z.P. Smith, R. Guo, L.M. Robeson, J.E. McGrath, D.R. Paul, B.D. Freeman, Energy-efficient polymeric gas separation membranes for a sustainable future: a review, Polymer 54 (18) (2013) 4729–4761, https://doi.org/10.1016/j.polymer.2013.05.075.
[142] S. Tul Muntha, A. Kausar, M. Siddiq, Progress in applications of polymer-based membranes in gas separation technology, Polym. Plast. Technol. Eng. 55 (12) (2016) 1282–1298, https://doi.org/10.1080/03602559.2016.1163592.
[143] F. Moghadam, H.B. Park, Two-dimensional materials: an emerging platform for gas separation membranes, Curr. Opin. Chem. Eng. 20 (2018) 28–38, https://doi.org/10.1016/j.coche.2018.02.004.
[144] Y. Shen, H. Wang, X. Zhang, Y. Zhang, MoS2 nanosheets functionalized composite mixed matrix membrane for enhanced CO2 capture via surface drop-coating method, ACS Appl. Mater. Interfaces 8 (35) (2016) 23371–23378, https://doi.org/10.1021/acsami.6b07153.
[145] D. Wang, Z. Wang, L. Wang, L. Hu, J. Jin, Ultrathin membranes of single-layered MoS2 nanosheets for high-permeance hydrogen separation, Nanoscale 7 (2015) 17649–17652, https://doi.org/10.1039/C5NR06321C.
[146] Y. Zhang, Q. Shi, Y. Liu, Y. Wang, Z. Meng, C. Xiao, K. Deng, D. Rao, R. Lu, Hexagonal boron nitride with designed nanopores as a high-efficiency membrane for separating gaseous hydrogen from methane, J. Phys. Chem. C 119 (34) (2015) 19826–19831, https://doi.org/10.1021/acs.jpcc.5b04918.
[147] Y. Wang, et al., Functionalized boron nitride nanosheets: a thermally rearranged polymer nanocomposite membrane for hydrogen separation, Angew. Chem. 130 (49) (2018) 16288–16293, https://doi.org/10.1002/ange.201809126.
[148] M. Emanet, Ö. Şen, M. Çulha, Evaluation of boron nitride nanotubes and hexagonal boron nitrides as nanocarriers for cancer drugs, Nanomedicine 12 (7) (2017) 797–810, https://doi.org/10.2217/nnm-2016-0322.
[149] E. Duverger, S. Balme, M. Bechelany, P. Miele, F. Picaud, Natural payload delivery of the doxorubicin anticancer drug from boron nitride oxide nanosheets, Appl. Surf. Sci. 475 (2019) 666–675, https://doi.org/10.1016/j.apsusc.2018.12.273.
[150] S. Feng, H. Zhang, T. Yan, D. Huang, C. Zhi, H. Nakanishi, X.D. Gao, Folate-conjugated boron nitride nanospheres for targeted delivery of anticancer drugs, Int. J. Nanomed. 11 (2016) 4573–4582, https://doi.org/10.2147/IJN.S110689.
[151] S. Feng, H. Zhang, S. Xu, C. Zhi, H. Nakanishi, X.D. Gao, Folate-conjugated, mesoporous silica functionalized boron nitride nanospheres for targeted delivery of doxorubicin, Mater. Sci. Eng. C 96 (2019) 552–560, https://doi.org/10.1016/j.msec.2018.11.063.
[152] X. Cao, A. Halder, Y. Tang, C. Hou, H. Wang, J.O. Duus, Q. Chi, Engineering two-dimensional layered nanomaterials for wearable biomedical sensors and power devices, Mater. Chem. Front. 2 (2018) 1944–1986, https://doi.org/10.1039/C8QM00356D.
[153] Y. Zhang, Y.N. Wang, X.T. Sun, L. Chen, Z.R. Xu, Boron nitride nanosheet/CuS nanocomposites as mimetic peroxidase for sensitive colorimetric detection of cholesterol, Sensor. Actuator. B Chem. 246 (2017) 118–126, https://doi.org/10.1016/j.snb.2017.02.059.
[154] W. Luo, T. Yang, L. Su, K.C. Chou, X. Hou, Preparation of hexagonal BN whiskers synthesized at low temperature and their application in fabricating an electrochemical nitrite sensor, RSC Adv. 6 (2016) 27767–27774, https://doi.org/10.1039/C5RA27234C.
[155] K.B. Kim, W. Jang, J.Y. Cho, S.B. Woo, D.H. Jeon, J.H. Ahn, S.D. Hong, H.Y. Koo, T.H. Sung, Transparent and flexible piezoelectric sensor for detecting human movement with a boron nitride nanosheet (BNNS), Nano Energy 54 (2018) 91–98, https://doi.org/10.1016/j.nanoen.2018.09.056.
[156] S. Nagarajan, H. Belaid, C. Pochat-Bohatier, C. Teyssier, I. Iatsunskyi, E. Coy, S. Balme, D. Cornu, P. Miele, N.S. Kalkura, V. Cavailles, M. Bechelany, Design of boron nitride/gelatin electrospun nanofibers for bone tissue engineering, ACS Appl. Mater. Interfaces 9 (39) (2017) 33695–33706, https://doi.org/10.1021/acsami.7b13199.
[157] C. Gautam, D. Chakravarty, A. Gautam, C.S. Tiwary, C.F. Woellner, V.K. Mishra, N. Ahmad, S. Ozden, S. Jose, S. Biradar, R. Vajtai, R. Trivedi, D.S. Galvao, P.M. Ajayan, Synthesis and 3D interconnected nanostructured h-BN-based biocomposites by low-temperature plasma sintering: bone regeneration applications, ACS Omega 3 (6) (2018) 6013–6021, https://doi.org/10.1021/acsomega.8b00707.
[158] H. Belaid, S. Nagarajan, C. Barou, V. Huon, J. Bares, S. Balme, P. Miele, D. Cornu, V. Cavailles, C. Teyssier, M. Bechelany, Boron nitride-based nanobiocomposites : design by 3D printing for bone tissue engineering, ACS Appl. Bio Mater. 3 (4) (2020) 1865–1874, https://doi.org/10.1021/acsabm.9b00965.
[159] Y. Zhu, N.S. Hosmane, Nanostructured boron compounds for cancer therapy, Pure Appl. Chem. 90 (4) (2018) 653–663, https://doi.org/10.1515/pac-2017-0903.
[160] M. Kıvanç, B. Barutca, A.T. Koparal, Y. Göncü, S.H. Bostanci, N. Ay, Effects of hexagonal boron nitride nanoparticles on antimicrobial and antibiofilm activities, cell viability, Mater. Sci. Eng. C 91 (2018) 115–124, https://doi.org/10.1016/j.msec.2018.05.028.
[161] S. Mateti, C.S. Wong, Z. Liu, W. Yang, Y. Li, L.H. Li, Y. Chen, Biocompatibility of boron nitride nanosheets, Nano Res. 11 (2018) 334–342, https://doi.org/10.1007/s12274-017-1635-y.
[162] S. Pandit, K. Gaska, V.R.S.S. Mokkapati, S. Forsberg, M. Svensson, R. Kadar, I. Mijakovic, Antibacterial effect of boron nitride flakes with controlled orientation in polymer composites, RSC Adv. 9 (2019) 33454–33459, https://doi.org/10.1039/C9RA06773F.
[163] X. Li, X. Wang, J. Zhang, N. Hanagata, X. Wang, Q. Weng, A. Ito, Y. Bando, D. Golberg, Hollow boron nitride nanospheres as boron reservoir for prostate cancer treatment, Nat. Commun. 8 (2017), 13936, https://doi.org/10.1038/ncomms13936.